Universidade de Aveiro Departamento de Química
Ano 2014

GUILAINE MARQUES JARIA

ADSORÇÃO DE FLUOXETINA A CARVÕES DE BIO-RESÍDUOS ATIVADOS

ADSORPTION OF FLUOXETINE ONTO WASTE-BASED ACTIVATED CARBON

Universidade de Aveiro Departamento de Química
Ano 2014

GUILAINE MARQUES JARIA

ADSORÇÃO DE FLUOXETINA A CARVÕES DE BIO-RESÍDUOS ATIVADOS

ADSORPTION OF FLUOXETINE ONTO WASTE-BASED ACTIVATED CARBON

Dissertação apresentada à Universidade de Aveiro para cumprimento dos requisitos necessários à obtenção do grau de Mestre em Química, ramo de Química Analítica e Qualidade, realizada sob a orientação científica da Doutora Vânia Maria Amaro Calisto, Pós-Doc do Departamento de Química da Universidade de Aveiro, e do Doutor Valdemar Inocêncio Esteves, Professor Auxiliar do Departamento de Química da Universidade de Aveiro.

Aos meus pais e irmã, pelo incansável apoio

o júri

presidente	Prof. Doutor Artur Manuel Soares da Silva Professor Catedrático do Departamento de Química da Universidade de Aveiro
	Prof. Doutora Olga Manuela Simão Filipe Professora Adjunta da Escola Superior Agrária de Coimbra
	Prof. Doutor Valdemar Inocêncio Esteves Professor Auxiliar do Departamento de Química da Universidade de Aveiro

agradecimentos

Ao meu orientador, Professor Valdemar Esteves pela oportunidade de trabalhar com o seu grupo de analítica e pela orientação científica ao longo do trabalho.

À Doutora Vânia Calisto agradeço toda a disponibilidade, apoio, paciência e ajuda, não esquecendo o valioso conhecimento e orientação científica ao longo do trabalho.

Às minhas colegas de laboratório pela disponibilidade em ajudar e pelos momentos de boa disposição.

Aos meus colegas e amigos que me acompanharam nestes dois anos de mestrado, pelos bons momentos que passamos juntos.

Aos meus amigos e à minha família, pela amizade e apoio demonstrado.

E, por fim, um agradecimento especial aos meus pais e à minha irmã por me terem encorajado e apoiado desde sempre.

palavras-chave

Carvão ativado; ativação química; fármacos; ambiente; adsorção; isotérmica de adsorção.

resumo

Os carvões ativados são uma das técnicas mais promissoras para a remoção de compostos orgânicos e inorgânicos presentes nas águas. Neste trabalho, foram produzidos três carvões ativados utilizando como precursor lamas primárias residuais provenientes da produção de papel. Foi utilizada a ativação química com KOH, NaOH e $ZnCl_2$, aplicando as mesmas condições de pirólise aos três carvões. A caracterização dos materiais obtidos foi feita por meio de análise de carbono orgânico total (TOC), espectroscopia de infravermelho com transformada de Fourier usando a técnica reflexão total atenuada (FTIR-ATR), *Proximate and ultimate analysis*, microscopia eletrónica de varrimento (SEM), porosimetria de mercúrio, isotérmicas BET e determinação do ponto de carga zero (PZC). Foram realizados estudos de adsorção iniciados pela cinética de adsorção e seguidos das isotérmicas, usando experiências em vaso fechado. Os estudos de cinética de adsorção mostraram que, na generalidade, todos os carvões produzidos apresentaram um tempo de equilíbrio semelhante, cerca de seis horas. As isotérmicas permitiram testar a capacidade de adsorção dos carvões produzidos para o composto fluoxetina-HCl. Estes dois estudos foram também aplicados à lama primária pirolisada sob as mesmas condições mas sem ativação e também a um carvão ativado comercial, usado como referência. Entre os materiais produzidos, o carvão ativado com $ZnCl_2$ é o que apresenta uma área superficial específica (S_{BET}) superior e maior percentagem de carbono. A capacidade máxima de adsorção ($mg\ g^{-1}$) foi de 96.2 ± 1.0 para o PBFG4; 120.4 ± 2.5 para PS800-10; 191.6 ± 4.8 para PS800-10KOH; 136.6 ± 9.6 para PS800-10NaOH; e 28.4 ± 0.3 para PS800-10$ZnCl_2$. As isotérmicas obtidas apontam para a existência de diferentes mecanismos de adsorção entre os carvões, provavelmente devido aos seus valores de PZC.

keywords

Activated carbon; chemical activation; pharmaceuticals; environment; adsorption; adsorption isotherms.

abstract

Activated carbons are one of the most promising techniques for the removal of organic and inorganic compounds from waters. In this work three activated carbons were produced using as precursor primary paper mill sludge. Chemical activation was performed using three different activation agents, KOH, NaOH and $ZnCl_2$, and the same pyrolysis conditions were applied. The characterization of the obtained materials was made by means of total organic carbon analysis (TOC), Fourier infrared spectroscopy with attenuated total reflectance (FTIR-ATR), proximate and ultimate analysis, scanning electron microscopy (SEM), Hg porosimetry, BET isotherms and point of zero charge (PZC) determination. Adsorption studies were made, beginning with adsorption kinetic and then adsorption equilibrium (isotherms of adsorption), all performed in batch experiments. Generally, the carbons presented an equilibrium time of around six hours. Equilibrium studies allowed test the adsorption capacity of the produced carbons for fluoxetine-HCl. These two studies were also performed to the primary sludge pyrolysed under the same conditions without activation and also to a commercial activated carbon as reference. Among the produced materials, the carbon activated with $ZnCl_2$ has the higher BET surface area and percentage of carbon. The maximum adsorption capacity (mg g^{-1}) was of 96.2 ± 1.0 for PBFG4; 120.4 ± 2.5 for PS800-10; 191.6 ± 4.8 for PS800-10KOH; 136.6 ± 9.6 for PS800-10NaOH; and 28.4 ± 0.3 for PS800-10$ZnCl_2$. The isotherms obtained point for different mechanism of adsorption between the carbons, probably due to their distinct PZC.

CONTENT

LIST OF FIGURES

LIST OF TABLES

1. INTRODUCTION

1.1. IMPORTANCE OF THE ACTIVATED CARBONS

In drinking water more than eight hundred organic and inorganic chemicals have been identified, most of them are pollutants which are able to cause serious human diseases (Bansal and Goyal, 2005). These compounds can be derived from human activities such as the municipal and industrial wastewater discharges, rural and urban runoff and wastewater leaching, or may also originate from the natural decomposition of plant and animal matter. Due to the high population density, it is necessary to find processes that make possible the removal of these compounds from contaminated waters. Among the various existent remediation processes, we can highlight those based on coagulation, oxidation, ion exchange and adsorption on activated carbon. The use of activated carbon seems so far to be one of the most promising way of removing contaminants from contaminated environments (Bansal and Goyal, 2005).

The origin of the use of activated carbon is not well defined, however, it is known that prior to using what is now called activated carbon, it was used carbon materials from vegetable origin (wood) as adsorbents. The first uses of such materials date from 3750 BC, Egypt and Sumer, where coal was used for the reduction of copper and tin ores for the production of bronze. In 1550 AC it was used for the first time in Greece for medicinal purposes. The application of carbon for water filtration dates from around 400 BC, in order to eliminate the taste and odor of it and to prevent diseases. The first industrial application was incorporated in England in 1794, in the sugar production industry as a bleaching agent. This event marks the beginning of research on activated carbon used in liquid phase (Bandosz, 2006).

The concept of adsorption, closely linked to the use of activated carbon, was first mentioned in the context of capture of gases by charcoal, in 1881. For this same time, R. von Ostrejko found what we now call activated carbon, patenting two methods of production of the same, namely, by the carbonization of lignocellulosic materials with metal chlorides, which is basically the current chemical activation, and gasification of coal with carbon dioxide or water vapor, known as physical or thermal activation (Bandosz, 2006).

In World War I there was great progress in the production and application of activated carbons, for example, in the development of gas masks, in water treatment and removal of vapors from the gas phase. Also, in the second half of the last century, the imposition of strict regulations on the environment related to water resources, application of clean gases and chemicals economic recovery has boosted production and use of activated carbons.

Professor Harry Marsh stated about activated carbons:
"Activated carbon is the Cinderella of the Carbon family, (...) and after purifying tonnes of sugar, cleaning up oceans of water, and enormous Amounts of food, (...), they were never taken to the Ball." With this sentence, Harry Marsh tried to show the importance of the activated carbons for society (Bandosz, 2006).

One of the positive aspects of the evolution of society is the development of products, methods and techniques which predicate the improvement of quality of life. However, there is also a negative aspect of this evolution which is the fact of involving big changes in everyday people life which in some cases, result in stress and other psychiatric disorders as, for example, depression. Often, these conditions are treated through the use of drugs in particular through the consumption of antidepressants (Nabais et al., 2008). The detection of pharmaceutical compounds in several environmental compartments has been increasing not only because of the high consumption patterns but also due to the improvement in detection methods (Bell et al., 2011). The concentrations of these pharmaceuticals (antidepressants) in the aquatic environment are very low, appearing between the nanogram-per-liter (of $ng.L^{-1}$) to microgram-per-liter ($\mu g.L^{-1}$) and not representing itself an immediate toxicological hazard to humans or to other living beings. However, the presence of these compounds may have additive and synergistic effects and can even become persistent leading to accumulation, as in the case of antidepressants (Bell et al., 2011; Calisto, 2011).

This cumulative and continuous contamination can become harmful not only to animals and plants which are part of the aquatic environment but also for humans who daily consume contaminated water. Thus, the presence of these and other drugs in aquatic environments is one of the emerging issues in environmental studies, making it necessary to develop effective and cost effective treatment methods for water. The graph in Figure 1 shows the number of different psychotropic antidepressants packaging distributed by the National Health System in Portugal, from 2007 to 2011. It is clearly showed the increase in the number of packages, in particular drugs containing fluoxetine. It should be noted, though, that fluoxetine occupied in 2011, the 39 place in the ranking of 100 most active substances consumed in Portugal.

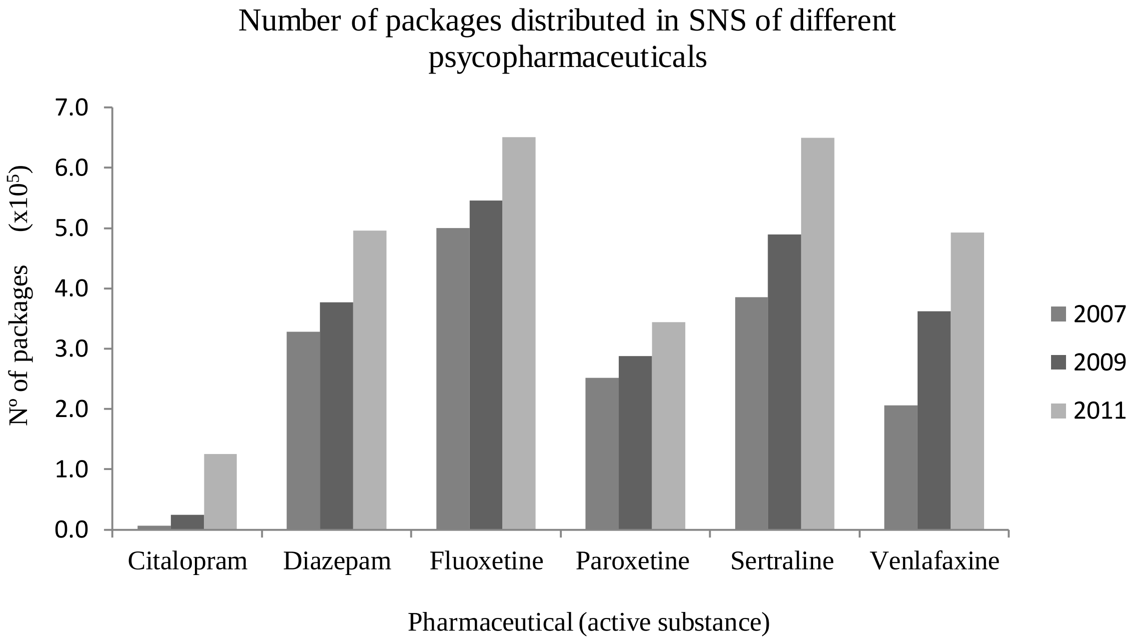

Figure 1 – Comparative graph of the number of packages sold in Portuguese National Health Systems containing active substances with antidepressant action (Infarmed statistics of medicine 2007, 2009 and 2011) (Infarmed)

Fluoxetine is a chemical compound belonging to the family of antidepressants called Selective Serotonin Reuptake Inhibitors (SSRI’s). It is the most widely used compound for treatment of mental depression and it is also used to treat obsessive-compulsive disorder, being present in the drug trademark Prozac (Flores et al., 2005; Nabais et al., 2008).

Typically, the molecule used for the pharmaceutical formulation of the drug is fluoxetine-HCl, whose name according to IUPAC is N-methyl-3phenyl-3-[4 -(trifluoromethyl) phenoxy] propan-1-amine hydrochloride with the molecular formula $C_{17}H_{18}F_3NO \cdot HCl$. The structures of the enantiomers of fluoxetine are shown in Figure 2.

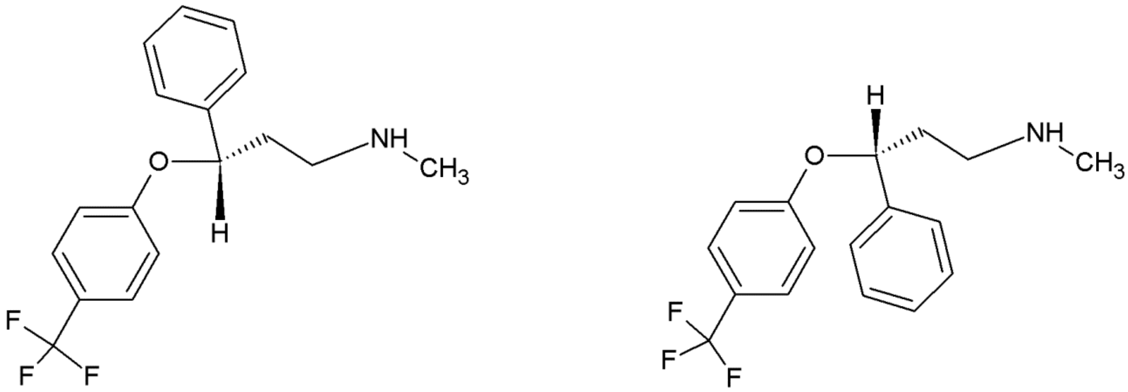

(a) S – Fluoxetine

(b) R – Fluoxetine

Figure 2 – Molecular structure of fluoxetine

Fluoxetine was reported as being one of the most persistent pharmaceuticals from the SSRI group, even after some treatments as chlorination (Lichtfouse et al., 2012). The development of methods for the efficient treatment of waters that are simultaneously efficient and low cost are still a challenge, therefore is important continuing to explore this area, for instance, in the production of specific adsorbent. Some studies that have been made about the removal of fluoxetine by adsorption are presented in Table 1.

Table 1 – Methods for removal of fluoxetine from water presented in literature

Adsorbent	Quantification method	% of Removal / adsorption capacity (mg g^{-1})	Reference
Activated charcoal (Norit USP XXIII)	ultraviolet absorption (spectrometer)	258 (pH 1.2) mg g^{-1} and 330 (pH 7.5) mg g^{-1}	(Cooney and Thomason, 1997)
Activated charcoal Commercial Activated carbon : Carbomix	Ion-selective electrode (ISE) potentiometry	--	(Atta-Politou et al., 2001)
commercial activated carbons (carbomix and maxsorb) one activated carbon fibre three MCM-41 samples	ultraviolet absorption (spectrometer)	Adsorption capacity between 55 and 1112 mg g-1	(Nabais et al., 2008)
activated carbon carbonaceous resin two high-silica zeolites	LC/MS/MS	98.4 % 78.8 % < 25 %	(Rossner et al., 2009)
Activated sludge (CAS) Hollow-fibre (FS) MBR Flat-sheet (FH) MBR	HPLC	33.1 ± 28.9 % 98.0 ±1.9 % 98.0 ±1.6 %	(Radjenovic et al., 2009)
Sodium dodecyl sulfate (SDS) coated Fe3O4 nanoparticles (NPs)	magnetic solid phase extraction (MSPE) and spectrofluorimetry	80 %	(Bagheri et al., 2011)
crosslinked β-cyclodextrin-carboxymethylcellulose (β-CD-CMC) polymer	ultraviolet-visible (UV-vis) and Fourier transform infrared (FTIR) spectroscopies	5.076 mg g^{-1}	(Bonenfant et al., 2012)

1.2. ACTIVATED CARBON

1.2.1. Definition and applications for activated carbon

A peculiarity of carbon materials is the easiness in controlling their properties. The different organizations or groups of segments of carbon atoms in such materials provide an extremely wide range of physical, chemical and mechanical properties. No other material has this feature and that is what makes their wide applicability in various industrial practices (Marsh and Rodríguez-Reinoso, 2006).

Activated carbon, such as carbon materials in general, is a porous carbonaceous material derived from a carbonaceous starting material. However, the activated carbon is subjected to a treatment with gas or chemical agents before, after or during carbonization in order to increase its adsorptive properties by increasing its porosity and improving chemical surface properties. It is a material which has a high adsorption capacity, preferably for small molecules and, therefore, is widely used for the purification of liquids and gases, in particular for water and air treatment and also for separating gaseous mixtures (Alcañiz-Monge and Illan-Gomez, 2008; Azargohar and Dalai, 2006; Bandosz, 2006; Guo and Rockstraw, 2006; IUPAC, 2012; Junior, 2004; Marsh and Rodríguez-Reinoso, 2006; Srinivasakannan and Bakar, 2004). Activated carbons were the first adsorbents to be developed. They are produced from a carbonaceous starting material that is designated as a precursor, which is transformed or activated by using a high temperature treatment, responsible for removing solid mass and simultaneously pores are created in the places where the mass was removed. A common property of activated carbon and other carbon adsorbents is their well-developed porous network (Bandosz, 2006). In fact, the term activated carbon refers to the porosity contained within the material constituting carbon (Junior, 2004; Marsh and Rodríguez-Reinoso, 2006).

Activated carbons have surface areas in the range of 500-3000 m^2 g^{-1}. The porous structure of the carbons and their surface chemistry determine their properties and are influenced by the nature of the used raw materials and the methods of carbonization and activation (Bandosz, 2006; Dabrowski et al., 2005).

There are several sources that can give rise to activated carbons and the same source can originate activated carbons with different properties only by altering and controlling the processes of carbonization and activation. The most commonly reported precursor materials in the literature are wood, coconut shell, fruit seeds, charcoal, lignin and synthetic macromolecular systems (Dabrowski et al., 2005; Marsh and Rodríguez-Reinoso, 2006; Srinivasakannan and Bakar, 2004). The starting material is chosen according to certain characteristics, such as: low content in inorganic matter, simple activation, high availability and low cost and low degradation during storage, and the purpose for which it is intended the activated carbon (Dabrowski et al., 2005).

One of the starting materials which can also be used to produce the activated carbon is biomass. When the biomass used for the production of activated carbon is of the lignocellulosic type, the name given to the product of the fast pyrolysis of biomass is biochar (Kim et al., 2012). Currently, much attention has been given to the use of biochars to water and air purification, since it is a renewable resource (Karakoyun et al., 2011).

The production of activated carbons involving lower costs and obtained from renewable sources is of great importance because the commercial activated carbons that are used as adsorbents in the removal of contaminants from wastewater are expensive materials. Therefore, it is necessary to develop less costly methods of producing activated carbon, which can be achieved using biomass materials as precursors of biochar, for example, primary sludge from paper pulp production, which will be the precursor used in this study.

1.2.2. The carbon element and the production of carbon materials

The carbon materials are mainly composed by the carbon element that has unique characteristics due to its electronic configuration ($1s^2\ 2s^2\ 2p^2$) (Bandosz, 2006; Marsh and Rodríguez-Reinoso, 2006). There are three major carbon allotropic forms: diamond, graphite and fullerenes, which depend on the type of binding/hybridization between the carbon atoms. The most common form is graphite with a sp^2 structure, being the most stable form and with less free energy so that most forms of carbon after heat treatment, tends to approach the allotropic structure of graphite. This process is called graphitization. Thus, the precursor materials after heat treatment give rise to carbons that are in the allotropic form of graphite. These materials can be categorized into graphitic and non-graphitic carbons, terms that are associated with their crystallographic order. The activated carbons ("chars") are classified as non-graphitic because they have disordered microstructures. The non-graphitic carbon can be further divided into graphitizable carbons (anisotropic) and non-graphitizable (isotropic) depending if after thermal treatment (above 2000°C) they are able or not able to be converted to a graphitic carbon, respectively (Bandosz, 2006; Marsh and Rodríguez-Reinoso, 2006).

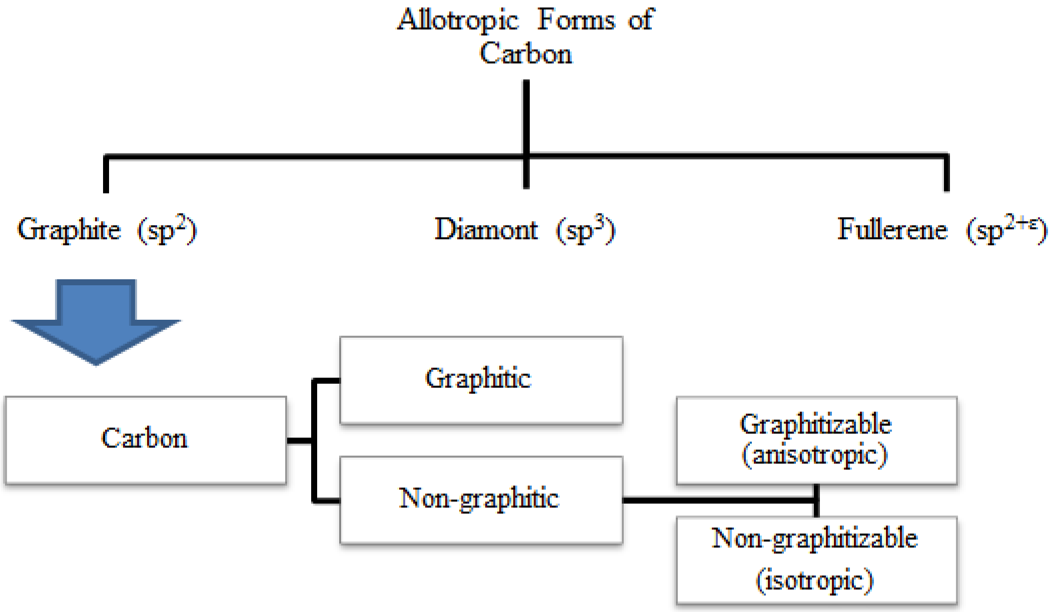

Figure 3 – Schematic representation of the carbon forms

Precursors from which activated carbons are produced are non-graphitic and non-graphitizable carbonaceous materials having an isotropic initial structure. These precursors which will undergo carbonization are generally organic materials (macromolecular systems) that go through to elevated temperatures suffering decomposition, involving the release of gaseous and liquid low molecular weight compounds. That is, a "pseudo-amorphous" carbon is formed which has a similar shape to that of the precursor material but having a lower density. The decomposition of the starting material ends upon the finish of the heat treatment and the greater the temperature more stable structures are formed. The temperature is then a decisive parameter for the structure of the final carbon. The decomposition process that occurs during the carbonization involve the movement of carbon atoms in short distances (it is presumed that those are smaller than 1 nanometer) within the macromolecular network to positions of greater stability, resulting in the formation of six membered ring systems. Eventually, a network of carbon atoms is created with residual hydrogen atoms attached to them, which form the structure of carbon materials. Each precursor will undergo a characteristic decomposition giving rise to a particular carbon. In this process free spaces of atomic dimensions are formed that were occupied by heteroatoms which are released in the form of volatile or due to migration and cross-linkage of atoms of carbon to form a network, constituting the carbon main feature: porosity (Bandosz, 2006; Marsh and Rodríguez-Reinoso, 2006).

From the industrial point of view this kind of carbonization (called solid phase) are performed using lignocellulosic precursors and coals, giving rise to non-graphitizable carbons (isotropic) with high microporosity (Bandosz, 2006; Marsh and Rodríguez-Reinoso, 2006).

1.2.3. Characterisation of activated carbons

1.2.3.1. Structure and porosity

The structure and porosity of a coal are two characteristics that are closely linked, as the presence of porosity in the activated carbon is due to the organization of its structure. In turn, this porosity is the one responsible for the dominant adsorption properties that are presented by activated carbons. All this implies that to use effectively an activated carbon is necessary to know its origin and preparation method, since these are the two factors that influence its structure (Marsh and Rodríguez-Reinoso, 2006). Knowing the structure of graphite helps to understand the structure of an activated carbon.

a) Graphite

As mentioned above, most of the structures of all known forms of carbon , with the exception of the diamond shape, are associated with graphite , presenting a decrease in the order degree of a hexagonal crystal of graphite to the more disordered porous carbon and amorphous. Graphite consists in layers of graphene, that is, layers of hexagonal arrangements of carbon atoms. These layers are ordered in parallel in a sequence ABABAB having a distance between layer of 0,335 nanometers (nm). Within each layer, linked atoms are separated by 0.142 nm and the bonds are σ trigonal with sp^2 hybridization, existing delocalized π bonds. It is noted that the value of 0,142 nm is between the values of the connections for $C(sp^3)$—$C(sp^3)$ (0.153 nm) and the values of the connections for $C(sp^2)$—$C(sp^2)$ (0.132 nm). In addition, the bond length of 0.142 nm is less than the interlayer distance which means that between the layers it has no formation of chemical bonds, only existing van der Waals forces (Bandosz, 2006; Marsh and Rodríguez-Reinoso, 2006).

In the case of diamond, the absence of layers similar to graphene causes the impossibility of having a porous structure. It is important to refer the diamond because there are suggestions that in the activated carbons the carbon atoms, which have an inherent porosity, may contain sp^3 linkages (Marsh and Rodríguez-Reinoso, 2006).

The activated carbon presents, similarly to graphite, a microcrystalline structure. However, there are some differences among them in particular with regard to the interlayer space, which in the case of activated carbon is between 0.34 and 0.35 nm, and in the orientation of the aromatic sheets, which are less ordered on activated carbon (Marsh and Rodríguez-Reinoso, 2006).

b) Activated Carbon

When it is desired to obtain an activated carbon, the precursor material, which is carbonized in an inert atmosphere, tends to have a structure close to the one of graphite after pyrolysis, that is, there are formed structures that can be considered as segments (non-three-dimensional) of graphene sheets. These segments will have different sizes, reaching the order of nanometers, cavities, absence of flat surface, linear carbon atoms ("dangling bonds" - sp^3 hybridization), presence of heteroatoms and will be connected together in an infinite number of shapes. These segments can be viewed as polycyclic aromatics compounds with various complex bonds forming a three-dimensional network of carbon atoms including carbon atoms with sp^3 bonds. It is the random connection of the carbon atoms of the defective polycyclic groups with linear carbon atoms that creates the porosity of the carbon, that is, spaces created due to imperfect packing (Bansal and Goyal, 2005; Marsh and Rodríguez-Reinoso, 2006).

In general, it appears that the carbon sheets are made of condensed polyaromatic sheets which have at their ends heteroatoms. These heteroatoms will define some characteristics of the activated carbon and thus may also play an important role in the adsorption process. In addition, this structure is also a free radical structure or with unpaired electrons that are stabilized by resonance and trapped during the carbonization process due to cleavage of bonds in the border of the aromatic sheets (Bansal and Goyal, 2005; Marsh and Rodríguez-Reinoso, 2006; Patricia et al., 2002).

The organization of the graphene layers of different classifications of carbons, and then its structure, is schematically represented in figure 4. In the case of Figure 4 (a) , the carbon was easily graphizated and graphene layers are parallel; in the case of Figure 4 (b), units that are not flat, establish connections during their formation during carbonization, which results in carbon with a low degree of graphitization. Heating up to 2000°C cannot change this organization, since it would then need to break many links simultaneously and overcome extremely high activation energies (Bansal and Goyal, 2005; Marsh and Rodríguez-Reinoso, 2006).

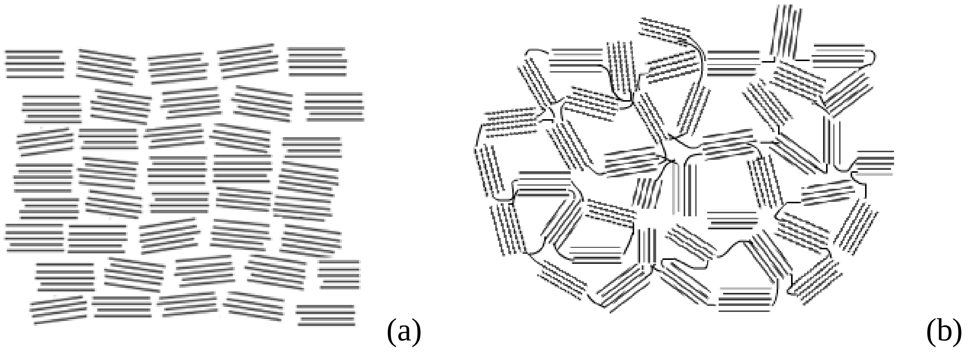
(a) (b)

Figure 4 – Schematic representation of grafitizable carbon (a) and non-grafitizable (b), based on the drawings adapted from Franklin Marsh and Rodríguez-Reinoso (2006).

As already mentioned, activated carbons have well-developed porous structure and a large specific inner surface. They consist mainly on carbon (87 to 97%) and other elements such as oxygen, hydrogen, sulphur and nitrogen. They might possess also other elements from the starting material and from the manufacturing process and also minerals and ash (inorganic matter). A typical activated carbon present a characteristic elemental composition of about 88% C, 0.5% N, 1.0%S and 6 to 7% O, being the remaining percentage associated with the inorganic ash. However, the percentage of oxygen varies depending on the starting material used and on the conditions of the activation process (Bandosz, 2006; Bansal and Goyal, 2005).

The pore size distribution and pore size are responsible for the high surface area of the activated carbon and, consequently, of the high adsorption capacity for organic and inorganic molecules. According to the International Union of Pure and Applied Chemistry (IUPAC), pores are classified as micropores, when smaller than 2 nm, mesopores for dimensions between 2 and 50 nm, and macropores larger than 50 nm. An activated carbon with a high microporosity has a high surface area. Thus, it is important that activated carbons have a large micropore volume with a pore size distribution appropriate so to have a large adsorption capacity and being capable of adsorbing molecules of different sizes. Also, it is important the existence of mesopores in proper proportion for facilitating the access to micropores. The macropores are not very important for the adsorption process but they can also act as transport channels for the adsorbate reach the meso- and micropores (Bansal and Goyal, 2005).

The higher the specificity of applications for what the activated carbon are intended, the greater control of pore size distribution is required, since with this control is possible, for instance, to adsorb and desorb molecules, distinguish kinetics of molecules with different size or even, “store” molecules (Chingombe et al., 2006; Marsh and Rodríguez-Reinoso, 2006).

1.2.3.2. Functional groups

Most applications of activated carbons are related to the presence of functional groups on its surface determining the chemical stability and the affinity of the adsorption process (Bandosz, 2006).

Generally, activated carbons own acidic and basic carbon-oxygen groups. Carboxyl, lactones and phenols groups, which make the carbon surface polar and hydrophilic, are considered as acidic groups. The basic groups are the ones like pyrones and chromenes structures (Figure 5) (Bansal and Goyal, 2005; Dabrowski et al., 2005; Patricia et al., 2002).

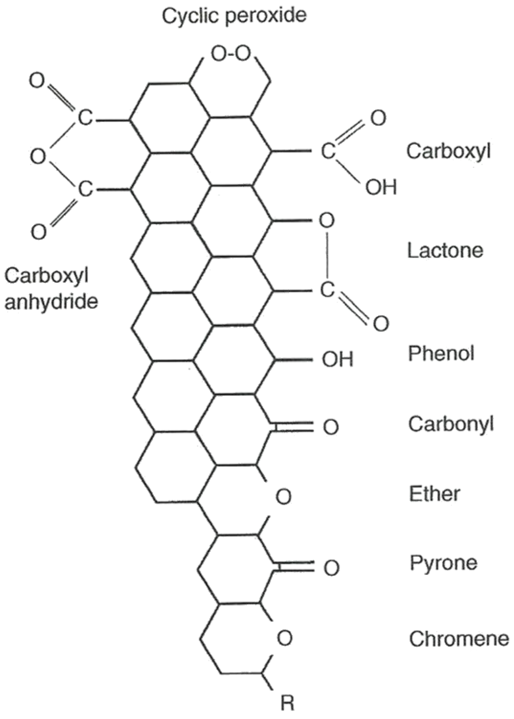

Figure 5 – Functional groups existing on the surface of a carbon (Marsh and Rodríguez-Reinoso, 2006)

These functional groups, not only influence the behaviour of the surface, water permeability, electrical or catalytic properties of the carbons, but also introduce the possibility to functionalize the surface of the activated carbon. This functionalization process open many doors for research aiming to solve a variety environmental problems (Bandosz, 2006; Patricia et al., 2002).

The nature and concentration of the surface charge of an activated carbon has also a central role in aqueous adsorption processes, being able to change it by modifying the pH of carbon-solution system. The surface charge of an activated carbon may be positive or negative depending if the pH of the system has a value below or above, respectively, the value of PZC (point of zero charge), that is, the value of pH where the total surface charge is zero. It is considered that the positive charge is related to the presence of basic groups on the surface, to excessive protonation of the surface at low pH values, and to graphene layers which act as Lewis bases (due to π delocalized electrons) resulting in the formation of donor-acceptor complexes important to the adsorption of many organic compounds in aqueous solution donor. The negative charge observed at high pH values is due to the ionization of the acidic groups which make the surface hydrophilic and polar (Bansal and Goyal, 2005; Patricia et al., 2002).

Since the organic compounds present in water may be polar or non-polar, interactions that will be present in the adsorption process may be electrostatic or dispersive. Moreover, hydrogen bonding can also be formed in some polar organic molecules (Bansal and Goyal, 2005; Patricia et al., 2002).

1.2.4. Production of activated carbons

1.2.4.1. Process steps

The process of producing an activated carbon involves two fundamental steps: carbonization and activation.

In the carbonization process, it takes place the elimination of most of the elements that are not carbon such as oxygen, hydrogen and nitrogen. These are volatilized by the initial pyrolytic decomposition. The residual elemental carbon atoms are grouped in flat layers, forming aromatic sheets randomly interconnected giving rise to an irregular arrangement of the same, responsible for the development of interstices/voids that give rise to porosity. Also, during the carbonization these pores are filled with heavy hydrocarbons or decomposition products or at least partially blocked with disordered carbon atoms. Generally, the carbonization process takes place at temperatures of around 800°C under inert atmosphere. The formed porous structure is strengthened and improved by the activation process which will allow greater random distribution of pores, which in turn will give rise to an extremely high surface area, reaching in some cases to 3000 m^2 g^{-1}. Depending on the chosen activation method, the activation step can be made before or after carbonization (Bansal and Goyal, 2005).

The development of porosity of an activated carbon is influenced by many experimental parameters related with the production process, in particular, the weight ratio between the precursor and the activating agent, the maximum activation temperature, residence time and nitrogen flow. The ratio between the activating agent and the precursor material is considered by many authors the factor that most influences the characteristics of the activated carbon (Alcañiz-Monge and Illan-Gomez, 2008; Azargohar and Dalai, 2008).

1.2.4.2. Chemical and physical activation methods

The main activation methods employed are chemical activation and physical activation (Bandosz, 2006). The method that was tested in the experimental approach of this work is the chemical activation.

a) Physical activation

The process of physical activation involves the carbonization of the starting material under an inert atmosphere followed by application of water vapour or carbon dioxide (CO_2), or a mixture of both, for gasification of the produced carbon under controlled conditions. The carbon gasification involves the removal of carbon atoms due to the reaction with the activating agents (water vapour and carbon dioxide) releasing carbon monoxide and hydrogen. It is a process that necessarily involves two steps, first the carbonization and then the activation with a gas and need very high temperatures. With this process, the porous structure is improved and the volatiles are removed leaving only carbon skeleton. A disadvantage of this method is that it cannot influence the micropore size distribution by manipulating experimental variables such as temperature, pressure and heating rate. However, this type of activation is quite used once it is generally applied to characterize the porosity of activated carbon (Dabrowski et al., 2005; Lillo-Rodenas et al., 2003; Marsh and Rodríguez-Reinoso, 2006).

b) Chemical activation

Chemical activation involves the addition of a chemical agent (activating agent) before the carbonization process (Bandosz, 2006). The parent material is impregnated with the activating agent prior to going through a process of pyrolysis (under inert atmosphere) and finally the produced carbon is washed for removal of excess of activating agent (Dabrowski et al., 2005; Junior, 2004). Although, generally the chemical activation is performed in one step, that is, the impregnation of the starting material (not charred) and then the carbonization (Hayashi et al., 2000; Tay et al., 2009), some authors suggest the impregnation of a precursor with an activating agent after a pyrolysis step, that is, the impregnation of a carbonized material. This process may be considered as having two stages, like physical activation (Azargohar and Dalai, 2008; Cao et al., 2006). However, the chemical activation process in two steps is not much found in the literature.

The main reagents used as activating agents, referred to in the literature, are zinc chloride ($ZnCl_2$) , phosphoric acid (H_3PO_4), potassium hydroxide (KOH) and sodium hydroxide (NaOH) (Azargohar and Dalai, 2006; Cao et al., 2006; Junior, 2004; Srinivasakannan and Bakar, 2004; Tay et al., 2009). These agents have the ability to decompose the cellulosic material during pyrolysis resulting in the charring of the material and in the increase of the aromaticity of the carbon structure (Dabrowski et al., 2005; Junior, 2004; Khalili et al., 2000).

The chemical activation process is still not fully understood. For example, in the case of chemical activation with potassium hydroxide two versions are commonly referred to explain the activation process. One version is the suggestion that the addition (*intercalation*) of potassium compounds in the carbonaceous structure is the main factor responsible for the development of porosity. Other version is that the activation process is due to gasification reactions between the KOH and the carbon material (Alcañiz-Monge and Illan-Gomez, 2008). The latter version is justified by the yields obtained from the production of activated carbon from lignocellulosic precursors by chemical activation with KOH, which is close to those obtained by physical activation. On the other hand, it is considered that the reagent used as the activating agent, may be incorporated within the particles so as to inhibit the contraction of the precursor material that occurs during the pyrolysis when the temperature rises, together with weight loss. This fact indicates that the reagent may act as a template for the creation of microporosity (Marsh and Rodríguez-Reinoso, 2006).

The reduction of metallic ions to alkali metal atoms leads some authors to consider that intercalation occurs in the activation process. The *intercalation* is a property of graphite that is associated, as its name indicates, to the assembling of elements between the graphene layers resulting in the expansion of the interlayer spaces. Apparently, potassium is an element that is readily intercalated; however, with sodium the intercalation does not happen easily. Apparently, sodium prefers to assemble inside less ordered carbons (non-graphitic). In the intercalation process alkali transference of electrons occurs from the metal to the π conduction band that exists between the graphene layers. Supposedly, it is the removal of these intercalated metals, by the temperature increase, that will determine the porosity of the final carbon (Alcañiz-Monge and Illan-Gomez, 2008; Marsh and Rodríguez-Reinoso, 2006). Therefore there are references about the differences between the use of NaOH and KOH with respect to the structural arrangement of the carbon. That is, the NaOH is said to be more effective for materials with a low structural order and KOH is better for materials with a high degree of order (Lillo-Ródenas et al., 2007).

However, although the mechanism of the activation process is not completely elucidated (Junior, 2004) according to some authors, the chemical activation using a hydroxide as activating agent seems to occur according to the following reaction:

$$6\ MOH + 2C \rightleftharpoons 2\ M + 3H_2 + 2M_2CO_3$$

Being M = Na or K. This reaction is an oxidation-reduction reaction in which the metallic cation undergoes reduction. The carbonate metal is one of the co-products formed during the process (Bandosz, 2006; Lillo-Ródenas et al., 2007; Tay et al., 2009).

In the case of using of zinc chloride as the activating agent, it acts as a dehydrating agent, promoting the decomposition of the precursor material during the pyrolysis process. In addition, zinc chloride also acts as a template, that is, when forming carbon part of this chemical remains in the interstices of the carbon, being removed using an extensive washing process of the activated carbon. Is this washing step that remove the zinc chloride that creates higher porosity (Khalili et al., 2000; Marsh and Rodríguez-Reinoso, 2006). The activated carbons prepared with zinc chloride are essentially microporous and the ratio(w/w) of zinc used has an important effect on the development of porosity and also in the micropores size distribution (Radovic, 2008). Zinc chloride is an activating agent that, until 1970, has been widely used, mainly for lignocellulosic precursor materials. However, it has some drawbacks such as low recovery efficiencies, corrosion problems, the presence of residual zinc in the carbon structure and the emission of metallic zinc, that may cause serious environmental problems. The strict control made to industrial emissions lead to the replacement of this chemical by phosphoric acid. Though, it appears that phosphoric acid limits the formation of tar and yields and high microporosity (Bandosz, 2006; Radovic, 2008).

The main differences between the use of KOH, H_3PO_4 and $ZnCl_2$ are related to the size of the porosity according to the ratio of the activation agent/precursor. For lignocellulosic starting materials, increasing the amount of KOH implies a greater microporosity and a broader size distribution of the micropores being negligible the amount of mesopores formed. Regarding $ZnCl_2$, there are development of both micropores and mesopores. In the case of H_3PO_4 essentially microporous are developed but with some formation of mesopores and macropores (Marsh and Rodríguez-Reinoso, 2006).

There are some advantages of chemical activation with respect to the physical activation, including higher yield, up to about 30% (w/w); lower pyrolysis temperatures are required; it is possible to obtain a larger surface area; pore sizes distribution is more easily controlled and maintained; and, the activation process is simpler, requiring no prior carbonization of the starting material. The main disadvantages are the use of chemicals which can be corrosive and affect the environment and also the fact that a final washing step of the product is required (Dabrowski et al., 2005; Junior, 2004; Lillo-Rodenas et al., 2003; Lillo-Ródenas et al., 2007; Tay et al., 2009).

1.2.5. Surface chemistry of activated carbons – functionalization

The possibility to modify the activated carbon surface in order to change and improve their adsorptive characteristics and make an activated carbon specific for a given application is one of the most interesting features of activated carbons. That is, even after the activation of a coal, it may be necessary to functionalize it for the formation of certain functional groups on the surface that interact with one or more specific compounds that one wants to adsorb. This process, which may be referred to as tailing is a way of introducing a specificity factor in the carbon that is to be produced. Thus, according to the functionalization, the carbon will adsorb only certain and specific adsorbates (Bandosz, 2006).

Changing the surface of coals consists, therefore, in the introduction of different functional groups in that material, and those groups will be formed depending on the type of treatment to which carbon is subjected. Some groups that can be obtained from certain treatments are presented in Table 2. These groups are attached to the corners or edges of aromatic sheets of the carbon changing the adsorptive capacity of the carbon, once those are the main part of the adsorptive surface (Bandosz, 2006).

In activated carbon there are areas in which are founded imperfections, flaws (voids in structural carbon, non-existence of aromatic rings). These areas with the ends of the carbon layers are referred to as active sites being associated with high densities of unpaired electrons, which imply a high tendency to adsorb chemically heteroatoms such as oxygen, hydrogen, nitrogen, sulphur, among others, giving rise to stable compounds on the surface of the carbon. Due to the high complexity of the surface of activated carbon, this should be treated as a whole and not as the sum of all individual functional groups in that area. The surface of activated carbon will influence the amphoteric character (acid or base) of the same (Bandosz, 2006).

Table 2 – Surface functional groups on activated carbons and respective treatment (Bansal and Goyal, 2005; Bandosz, 2006)

FUNCTIONAL GROUP	TREATMENT
Carbon-oxygen	Oxidation -Using gases or oxidant solutions - Heating at elevated temperature
Carbon-hydrogen	Hydrogenation -Treatment with hydrogen at high temperatures
Carbon-halogen (chlorine, bromide)	Halogenation -Treatment with gaseous halogens or in solution
Carbon-nitrogen	Nitrogenation - Reaction with nitrogenous compounds (ammonia, urea, melamine, hydrogen cyanide) - Preparation of a carbon whose precursor which contains considerable amounts of nitrogen element (acridine)
Carbon-sulphur	Sulfurization - Heating the carbon with elemental sulphur or sulphurous gases (CS_2, H_2S, SO_2)
Metals	- With metals or metal oxides.

The carbon-oxygen radicals are the most commonly found on the surface of an activated carbon. These groups are important for the acid-base characteristics of the carbons. The oxidation at elevated temperatures and with oxidizing agents in solution leads to acidification of the activated carbon. On the other hand, treatment at elevated temperatures removes compounds from the surface of the carbon, which leads to the formation of basic oxides (Bandosz, 2006; Bansal and Goyal, 2005).

The functionalization of activated carbons with halogens is done via physical and chemical adsorption, which may occur by:

- addition in unsaturated sites;
- exchange with chemically adsorbed hydrogen;
- oxidation of the carbon surface (Bandosz, 2006; Bansal and Goyal, 2005).

The type of process will depend on the nature of the activated carbon surface, on the amount of oxygen and hydrogen involved, on the experimental conditions and on the nature of the halogen species. For example, treatment with chlorine to modify carbons can be important when we want to have basic activated carbons. The reactivity of the halogen with coal decreases along the group of the periodic table (chlorine > bromine > iodine) (Bandosz, 2006; Bansal and Goyal, 2005).

Nitrogen existing in the surface of activated carbons plays a key role in the adsorptive properties of the same. At low temperatures nitrogen fixation is equivalent to the number of acidic groups containing oxygen and the carbon exhibits a slightly acidic character; at elevated temperatures substitution of the hydroxyl groups with amino groups occurs and also an increase of nitrogen atoms incorporated into graphitic layer in place of carbon atoms (Bandosz, 2006; Bansal and Goyal, 2005).

Sulphur is chemically adsorbed via connections with the peripheral carbon atoms, addition to unsaturated sites (with double bonds), penetration into the porous structure, and exchange by hydrogen or oxygen associated with the carbon surface (Bandosz, 2006; Bansal and Goyal, 2005).

Metals are associated to the change of the porous structure and of the characteristics of gasification (Bandosz, 2006; Bansal and Goyal, 2005).

The tailoring of the surface of activated carbons opens a wide range of possibilities so that can treat certain industry challenges, particularly in terms of catalytic processes, energy storage, remediation of aquatic environments, among others . It is an area that still has an enlarged open field in research studies (Bandosz, 2006) .

1.3. ADSORPTION AND THE STUDY OF REMOVAL OF PHARMACEUTICALS FROM WASTEWATERS

1.3.1. Adsorption

The study and production of solid adsorbents have been a constant over the years, particularly in respect to inorganic materials and carbonaceous materials (which include the coals). As the name suggests, adsorbent materials are materials that have a high adsorption capacity, representing an added value at technological, environmental and biological levels. The adsorption phenomenon is extremely important with regard to practical applications, namely, in industry practices, chemical processes based on adsorption, such as catalytic and separative methods (which may include water, air and soil purification) as well as pollution control and respiratory protection (Dabrowski, 2001; Rouquerol et al., 2014)

The adsorption has, therefore, a great technological importance being currently a well-established technique regarding the removal of organic compounds from water (drinking water, effluents and wastewater). The use of activated carbons is considered the most efficient and economic process for removing such organic compounds by adsorption, being one of the best technologies for environmental control (Foo and Hameed, 2010; Hamdaoui and Naffrechoux, 2007a; Rouquerol et al., 2014).

The adsorption process is a non-specific method. Occurs due to interactions between atoms or molecules of the solid and fluid phase, being a surface phenomenon in which molecules of a substance are attracted to and adhere to the surface of a solid phase, often called the condensed phase (Marsh and Rodríguez-Reinoso, 2006; Pereira, 2012). The definition of adsorption according to IUPAC is given as "an increased concentration of a dissolved substance in a condensed phase and a liquid or gas phase interface due to the action of surface forces" (IUPAC, 2012).

Adsorption is a spontaneous process, that is, to occur it is necessary that the free energy of adsorption, ΔG_{ads}, has a negative value. This free energy of adsorption depends, in turn, on electrostatic forces ("Coulomb" forces) related to the dissociation or protonation of the adsorbate (if it is an electrolyte) and non- electrostatic, which include van der Waals interactions, hydrophobic interactions and hydrogen bonds. These latter interactions are of physical nature, so when adsorption occurs due them, the adsorption process is designated as physical adsorption or physisorption. This type of adsorption is a reversible and exothermic process occurring with decrease of free energy and entropy. When the adsorption occurs by electrostatic forces is called chemical adsorption or chemisorption. The chemical adsorption occurs only in monolayer and some authors even consider that this type of process may involve valence forces through sharing or exchange of electrons (Bond, 1967; Dabrowski, 2001; Gregg and Sing, 1991; Ho, 2006; Marsh and Rodríguez-Reinoso, 2006; Moreno-Castilla, 2004; Pereira, 2012).

1.3.2. Adsorption isotherm

The fundamental concept of adsorption is expressed in the adsorption isotherms representing the equilibrium between the amount of adsorbed material, and the pressure or concentration of the fluid phase (liquid or gas) at a constant temperature. The isotherm is a distribution of potential adsorption along the carbon surface, which follows the Gaussian or normal distribution. Adsorption isotherms are essential for predicting, with a high degree of confidence, the adsorption parameters and the quantitative comparison of the behaviour of the adsorbent in different systems or in different experimental conditions. In water treatment processes using activated carbon, in order to be able to perform a quantitative analysis of the chemical compounds present in water that were adsorbed by activated charcoal, it is important to know the adsorption isotherm which allows determining the adsorption capacity that the activated carbon has for the compounds to be removed (Dabrowski, 2001; Foo and Hameed, 2010; Marsh and Rodríguez-Reinoso, 2006; Moreno-Castilla, 2004; Qi and Schideman, 2008).

In the literature, the concept of adsorption isotherm for activated carbon is often related to the adsorption of gases, because those are largely used for characterization of porosity of activated carbons. However, the concept of adsorption equilibrium of a gas is the same as for solutions, that is, when a gas is brought into contact with a solid, molecules/atoms of gas begin to be adsorbed by the surface of the solid. At first, the adsorption rate is higher because there is a lot of free surface. As the adsorption occurs and the surface starts to get filled, the reverse process (desorption) increasingly occurs while the adsorption rate decreases. When the rate of adsorption equals the rate of desorption, it is reached adsorption equilibrium, which will correspond to the maximum value that is adsorbed by the solid. In statistical terms, for the study of adsorption from dilute solutions, the equations of gas adsorption monolayer can be used by simply replacing the term pressure by the concentration of solution and modifying the dimensions of some parameters (Bansal and Goyal, 2005; Gregg and Sing, 1991; Moreno-Castilla, 2004).

As already indicated, the gas adsorption isotherms are generally used to characterize the adsorbent material with respect to its porosity and specific surface area, that is, the area per mass unit. However, isotherms of fluid-solid systems can also be used to determine the surface area of the solid, having the benefit of not requiring a vacuum system, as in the case of a gas-solid adsorption system, making it a faster and easier procedure (Bansal and Goyal, 2005; Moreno-Castilla, 2004; Pereira, 2012). In this study, the solid-liquid isotherms are used to study the adsorption equilibrium of fluoxetine between the solid phase (carbon) and the aqueous phase (aqueous solution of fluoxetine-HCl).

There are some differences between the adsorption in liquid-solid and gas-solid system, in particular because in the first case, considering dilute solutions, the adsorption process is an exchange process, that is, the adsorbed molecule can either be drawn by the solid from the solution or being rejected because, for example, of their hydrophobic properties. In addition, an aqueous solution is far from ideal and present adsorbate-adsorbate interactions which are negligible in comparison with the gases. Thus, the isothermal solid-liquid systems cannot exhibit an ideal shape and the multilayer adsorption is also less frequent than in gas-solid systems (Dabrowski, 2001; Moreno-Castilla, 2004).

To obtain an adsorption isotherm it is common to represent on the axis of ordinates the amount of solute adsorbed, which is an approximation, since it can either occur adsorption of the solvent or solute. Considering there is only solute adsorption, the equilibrium adsorption capacity is expressed as follows:

$$q_e = \frac{(C_0 - C_e)V}{m} = \frac{x}{m} \qquad \text{(equation 1)}$$

where:

C_0 - initial concentration of adsorbate in solution (mg L^{-1})

C_e - residual concentration of adsorbate in solution at equilibrium (mg L^{-1})

V - volume of solution (L)

m - mass of adsorbent (g) (Fuqiang et al., 2007)

x - amount of adsorbed solute (mg)

This equation (1) corresponds to the mass balance, at equilibrium, expressing the mass transfer of solute in the liquid phase to the solid surface which is represented by:

$$m(q_t - q_0) = V(C_0 - C_t) \qquad \text{(equation 2)}$$

in that q_t is the concentration of solute present in the solid at time t (mg g^{-1}), q_0 is the initial concentration of solute in the solid (usually zero) and C_t is the solute concentration in the liquid phase at time t (mg L^{-1}) and C_0 is the initial concentration of the solution (mg L^{-1}) (Bandosz, 2006).

Equation (2) is applied to the dilute solutions in which the variation of volume associated to the adsorption of solute can be neglected. Thus, the adsorption of solute is given by the variation between the initial and final weights (balance) of the adsorbate in the solution, given by the term $(C_0 - C_e)V$ present in equation (2). It appears that an increase in the concentration of solute in the solution implies an increase in capacity of adsorption equilibrium until a maximum value from which no more variation is observed (Pereira, 2012).

Various models of adsorption isotherms are reported in the literature, some of which may present itself as a bit complex due to structural heterogeneity and energy of most adsorbents (Dabrowski, 2001).

The knowledge of the adsorption process involves the understanding of two factors intrinsic to it, namely, the adsorption equilibrium and also the adsorption kinetics. The adsorption kinetics is an important factor because adsorption is not a process that is independent of time, therefore, being necessary to know the variation of adsorption rate (over time) in a solid adsorbent as a way to evaluate and designing this adsorbent for the intended use. In practice, having a good adsorbent require combining these two factors, that is, it is appropriate that the adsorbent can adsorb the most of the desired compound, but also it should do it in a feasible time interval. It is also important to note that absorption is directly related to desorption, being that fact very important regarding the regeneration of the adsorbent, which is a major problem associated with the use of activated carbon (Azizian, 2004).

1.3.2.1. Kinetics adsorption models

The adsorption kinetics includes the study of the adsorption of ions and organics in solution as well as gases. For kinetic studies, there are a wide variety of models which have been proposed by several authors. However, the most commonly used models are the pseudo-first order and pseudo-second order, being the ones applied in this work.

Pseudo-first order model

The pseudo-first order model, also called the *Lagergnen*, is based on the adsorption capacity of the solid and finds that there is a direct proportionality relationship between the rate variation of solute uptake over time and the difference between the amount adsorbed at equilibrium and the amount adsorbed at time *t*. Thus, the mathematical expression that describes the kinetics of adsorption of pseudo-first order model is presented as follows:

$$\frac{dq}{dt} = k_1(q_e - q_t) \qquad \text{(equation 3)}$$

being:

q_t – quantity of adsorbate removed at time t per unit mass of adsorbent (mg g^{-1})

q_e – adsorption capacity at equilibrium - mass of adsorbate per unit mass of adsorbent at equilibrium (mg g^{-1})

k_1 – rate constant of pseudo-first order (min^{-1}).

Integrating the above equation for the initial conditions $q_t = 0$ at $t = 0$ and $q_t = q_t$ at $t = t$ gives the equation

$$\ln(q_e - q_t) = \ln q_e - k_1 t \qquad \text{(equation 4)}$$

Whose nonlinear form is:

$$q_t = q_e[1 - \exp(-k_1.t)] \qquad \text{(equation 5)}$$

k_1 is the constant related to the rate of change of pseudo-first order equation and reflects a combination of the rate constants of adsorption k_a and desorption k_d, and is not intrinsic to the adsorption constant. The relationship between the constant k_1 and the rate constants of adsorption and desorption is expressed by:

$$k_1 = k_a C_0 + k_d \qquad \text{(equation 6)}$$

This is a linear function of the initial concentration of solute. Thus, analyzing the value of k_1 at various initial concentrations, it is possible to calculate the constant of adsorption (k_a) and desorption (k_d), and hence the equilibrium constant, K ($K = k_a/k_d$), by the graphical representation of k_1 vs C_0. The slope value will correspond to k_a and the intersection to k_d (Azizian, 2004).

Pseudo-second order model

The pseudo-second order model describes the behavior of the adsorption process in the whole range of contact time. It is expressed by the equation:

$$\frac{dq}{dt} = k_2(q_e - q_t)^2 \qquad \text{(equation 7)}$$

k_2 (g mg^{-1} min^{-1}) is a constant value that is a complex function related to the initial concentration of solute.

Integrating equation 7, we obtain:

$$q_t = \frac{k_2 q_e^2 t}{1+k_2 q_e t} \quad \text{(equation 8)} \qquad \text{or} \qquad \frac{t}{q_t} = \frac{1}{k_2 q_e^2} \cdot \frac{1}{q_e} t \quad \text{(equation 9)}$$

k_2 can be determined experimentally by plotting t/q_t versus t. It is also possible to define an initial rate of adsorption (for values close to zero), calculated using the expression: $h_0 = k_2 q_e^2$ (Ahmed and Dhedan, 2012; Azizian, 2004; Hameed et al., 2008; Machado, 2011; Qiu et al., 2009; Sekar et al., 2004).

1.3.2.2. Equilibrium adsorption models

As already mentioned, in general, an adsorption isotherm is a function that describes the process that governs the retention/release or movement of a substance from the aqueous medium to a solid phase at constant temperature and pH, since these two variables influence the adsorption phenomenon. The adsorption equilibrium is established when the adsorbate (in solution) remains long enough in contact with the adsorbent and implies that there is a dynamic balance between the concentration of adsorbate in the aqueous matrix and the concentration of the adsorbate in the interface. This equilibrium relationship which is established between the amount adsorbed and the amount remaining in solution is usually represented graphically, so it can be expressed by a mathematical expression. This mathematical expression is of the most importance for the analysis of models, operational planning and practical applications of adsorption systems (Foo and Hameed, 2010). Over the years many different isotherms have been proposed.

Isotherms can be divided into four main classes according to the initial slope, namely in S, L ("Langmuir" type), H ("high affinity"), and C ("constant partition" or Linear) isotherms (Giles et al., 1960; Limousin et al., 2007). Some authors also distinguish the F type that is, sometimes, considered as an L type isotherm and Butt et al. (2003) also refer a Step isotherm as being an H type isotherm (Figure 6). Giles et al. (1960) also divided the four main classes into sub-groups presenting one or two plateaus.

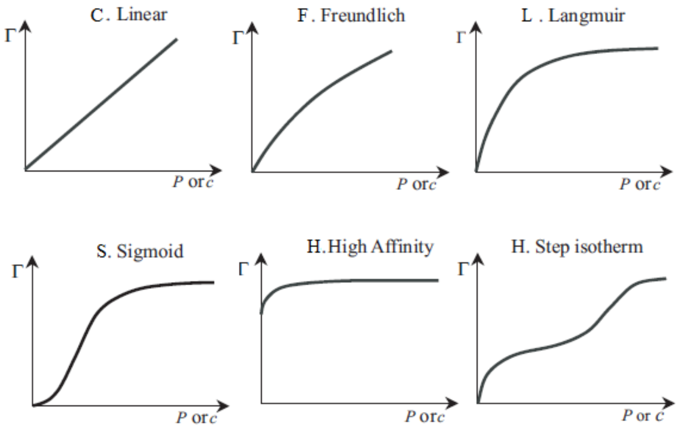

Figure 6 – Most common adsorption isotherms for adsorption of dilute solutions on carbon materials (Butt et al. (2003) and Moreno-Castilla (2004)).

Generally, the L type isotherms are the most frequently found in adsorption from dilute solutions, although sometimes S type isotherms can also be found and have been reported by some authors (Giles et al., 1960; Girods et al., 2009; Nevskaia et al., 2001). In L type isotherm, because a "plateau" is reached, it is considered that the adsorbed solute molecule is not vertically oriented, probably are adsorbed flat, and that there is no strong competition from the solvent. The solute molecule is equally stable wherever the site of adsorption (Giles et al., 1960).

In the initial stage of the normal L type isotherm, there are an increase in the adsorption capacity, because of the availability of the vacant sites, until saturation at high concentration, probably due to the surface being completely filled with solute molecules in a monolayer (Butt et al., 2003; Giles et al., 1960; Limousin et al., 2007). In S type isotherm the initial slope is different because the reverse conditions applies, that is, the adsorption of solute molecules facilitates the adsorption of additional amounts of solute due interactions between the adsorbate molecules, called “co-operative adsorption” (Butt et al., 2003; Giles et al., 1960; Limousin et al., 2007). According to Butt et al. (2003), flat and homogeneous adsorbents are required for this type of isotherms. H type isotherm is considered a special case of L type, presenting a vertical initial part that is assumed to be because of the high affinity to the solute, in dilute solutions, that is completely adsorbed (Butt et al., 2003; Giles et al., 1960; Limousin et al., 2007). This isotherm can also present two plateaus, being named of Step isotherm according to Butt et al. (2003). The first “plateau” corresponds to adsorption at the surface of the adsorbent and while the second “plateau” is due to de interactions between the adsorbed molecules as in S curve.

In this work, Langmuir, Freundlich, Redlich-Peterson, Sips or Langmuir-Freundlich, Hill, Zhu-Gu and MBET models used for fitting the experimental data. These models can be associated to L, S or H type isotherms. The equations and parameters associated with the respective models are outlined in Table 3. The expressions listed in the table are related to single component adsorption (Foo and Hameed, 2010).

Table 3 – Adsorption Isotherm models

Model	**Isotherm equation**	**Parameters**
Langmuir	$q_e = \frac{q_m K_L C_e}{1 + K_L C_e}$	q_m – maximum adsorption capacity (mg g^{-1}) K_L – equilibrium constant (k_1/k_2) related with the free energy of adsorption (L mg^{-1})
Freundlich	$q_e = K_F . C_e^{1/n}$	K_F- relative adsorption capacity (mg$^{1-1/n}$ L$^{1/n}$ g^{-1}) $K_F = \frac{q_m}{C_o^{1/n}}$ n – constant related with the degree of non-linearity of the equation (for n= 1, linear adsorption; n<1, non-favorable adsorption and n>1, favorable adsorption)
Redlich-Peterson	$q_e = \frac{K_{RP} C_e}{1 + \alpha_{RP} C_e^{\beta}}$	K_{RP} – affinity constant (L g^{-1}) α_{RP} –Redlich-Peterson isotherm constant (L mg^{-1}) β – parameter that varies between 0 and 1
Sips ou *Langmuir-Freundlich*	$q_e = \frac{q_m K_s C_e^{1/m}}{1 + K_s C_e^{1/m}}$	q_m - maximum adsorption capacity (mg g^{-1}) K_s – affinity constant related with the adsorption energy (L g^{-1}) m – parameter related with the heterogeneity of the system
Hill	$q_e = \frac{q_m (K_H C_e)^b}{1 + (K_H C_e)^b}$	q_m is the maximum adsorption capacity (mg g^{-1}) K_H - affinity parameter b - empirical parameter which varies with the degree of heterogeneity
Zhu-Gu	$q_e = q_\infty \frac{K_1 C_e (1/r + K_2 C_e^{r-1})}{1 + K_1 C_e (1 + K_2 C_e^{r-1})}$	q_∞ - associated to the limiting amount adsorbed at high concentration r - aggregation number K_1 - equilibrium constant for the adsorption interaction K_2 - equilibrium constant for the lateral interactions between adsorbed molecules
MBET	$q_e = q_m \frac{K_{MBET} C_e/C_o [1 - (s+1)(C_e/C_o)^s + s(C_e/C_o)^{s+1}]}{(1 - C_e/C_o)[1 + (K_{MBET} - 1) C_e/C_o - K_{MBET}(C_e/C_o)^{s+1}]}$	q_m - amount adsorbed in a complete monolayer K_{MBET} - equilibrium constant related to the adsorption energy C_o - saturation concentration of the solute in water s - number of layers
q_e - amount adsorbed at equilibrium (mg g^{-1}) C_e - equilibrium concentration of the adsorbate (mg L^{-1})		

(Ahmed and Dhedan, 2012; Bandosz, 2006; Bansal and Goyal, 2005; Debrassi, 2011; Desta, 2013; Foo and Hameed, 2010; Girods et al., 2009; Lima et al., 2011)

Langmuir isotherm model

Langmuir isotherm model implies a number of assumptions, including:

- Adsorption occurs in a monolayer, that is, the adsorbed layer has a thickness of a single molecule;
- The adsorption occurs at a finite number of identical and equivalent sites located in well defined spaces;
- Lateral interactions between the adsorbed molecules are considered to be negligible;
- Adsorption is homogeneous, that is, all adsorption sites have equal affinity for the adsorbate, being energetically equivalent.

The Langmuir isotherm model allows us to calculate the separation factor, R_L (equation 10), which indicates the degree of favoritism in the occurrence of adsorption (Foo and Hameed, 2010; Sekar et al., 2004):

$$R_L = \frac{1}{1+K_L C_e} \qquad \text{(equation 10)}$$

where:

- $0 < R_L < 1$: favourable adsorption
- $R_L = 0$: irreversible adsorption
- $R_L = 1$: linear adsorption
- $R_L > 1$: non-favourable adsorption

The Langmuir model is based on the assumption that the maximum adsorption corresponds to a saturated monolayer of solute molecules on the adsorbent surface. Thus, the mathematical expression of the isotherm yields a constant, q_m, which will be the maximum capacity of the adsorbent for a given solute. This constant corresponds to the *plateau* observed in the isotherm graph, which is characteristic of these isotherms. Often this value corresponds to the value of the monolayer (Bond, 1967; Gregg and Sing, 1991; Sekar et al., 2004).

Freundlich isotherm model

Freundlich model is an empirical model and according to the mathematical expression of this model, as the concentration of the adsorbate increases so does the concentration of adsorbate on the surface of the adsorbent, which is characterized graphically by the inexistence of a well defined plateau.

This model considers the adsorption as a reversible process and not ideal and it can occur either in monolayer or multilayer. The enthalpy of adsorption and affinity have a non-uniform distribution along the heterogeneous surface of the adsorbent (Foo and Hameed, 2010; Hamdaoui and Naffrechoux, 2007a; Sekar et al., 2004).

The parameter n indicates the degree of non-linearity between concentration of the solution and adsorption, such that if $n = 1$ it indicates that the absorption is linear. Therefore, this parameter allows to verify if the adsorption is favorable or unfavorable (Bandosz, 2006; Bansal and Goyal, 2005; Desta, 2013).

By the Freundlich equation it can be verified that q_e increases indefinitely with increasing C_e, which, in physical terms, is meaningless. Therefore, this equation is only valid for dilute solution, that is, solution with low concentrations.

Graphically, the differences between Langmuir and Freundlich isotherms are not many (Figure 7). In fact, the Freundlich isotherm is a limited form of the Langmuir equation. For gas-solid systems, the difference is that Freundlich isotherm is applied to mean vapor pressures (Bansal and Goyal, 2005).

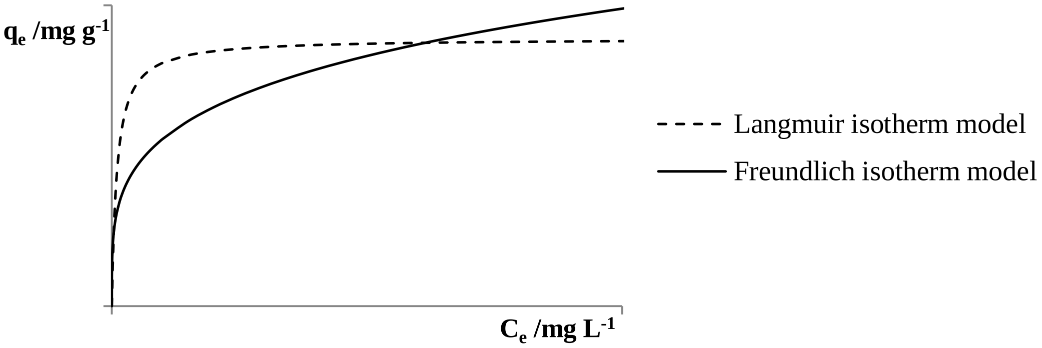

Figure 7 – Schematic representation of the isotherms of Langmuir and Freundlich

This type of isotherm also fits on type I isotherms of the Brunauer, Deming, Deming and Teller (BDDT) classification of (more commonly referred to as Brunauer, Emmett and Teller - BET), which is usually associated with the presence of microporosity in adsorbent (Bond, 1967; Gregg and Sing, 1991).

Redlich -Peterson isotherm model

Redlich-Peterson model isotherm is considered as a hybrid model comprising both characteristics of the Langmuir and the Freundlich isotherm. This model has three parameters and can be applied to homogeneous and heterogeneous systems. At high concentrations ($\beta \rightarrow 0$) the model approaches the Freundlich isotherm, for low concentrations ($\beta = 1$) the model is consistent with the ideal condition of Langmuir (Foo and Hameed, 2010; Hamdaoui and Naffrechoux, 2007b).

Sips or Langmuir- Freundlich isotherm model

The Sips isotherm model similarly to the Redlich-Peterson model is regarded as a model which combines the Langmuir and Freundlich isotherms. This model considers the adsorption in heterogeneous systems and circumvents the limitation of the Freundlich model to increase the associated concentration of adsorbate. Contrary to Redlich-Peterson model, Sips isotherm at low concentrations reduces itself to the Freundlich isotherm and at high concentrations provides a monolayer adsorption capacity characteristic of the Langmuir model (Ahmed and Dhedan, 2012; Foo and Hameed, 2010).

The parameters associated to the model equation are primarily managed by operational conditions, such as pH changing, temperature and concentration (Ahmed and Dhedan, 2012; Foo and Hameed, 2010).

Hill model

Hill isotherm model is also L type isotherm and a projection of Langmuir-Freundlich isotherm when the b parameter takes values higher than 1. This b parameter has the same meaning than the *n* in Freundlich isotherm. This model assume that the adsorbent surface is homogeneous and that cooperative effects can be present due to adsorbate-adsorbate interactions (Lima et al., 2011).

Zhu-Gu model

ZhuGu isotherm model is related with surface aggregate formation and is mainly applied to surfactants. According to this model the adsorption mechanism involve two coincident processes: first, the adsorption of molecules at the surface (interactions between the adsorbate molecules and the surface of the adsorbent) and second the interaction between adsorbed molecules (through hydrophobic interactions) (Girods et al., 2009; Zhu and Gu, 1989).

Modified BET (MBET) model

MBET isotherm is a modified BET isotherm applied to a finite number of layers in contrast with the BET isotherm that is applied to an infinite number of layers (Girods et al., 2009).

The study of the adsorption isotherms is important because allow us to describe how the organic compounds, in this case the pharmaceutical fluoxetine, interact with the adsorbent material, which is extremely important for the optimization of the adsorption mechanisms, expression of surface properties and characteristics and capabilities of the adsorbents (Foo and Hameed, 2010).

1.3.3. Adsorbate and adsorbent features

Adsorption is a process which, as already mentioned, depends on certain features of the adsorbent, in this case of the activated carbon, but also depends on the adsorbate.

In a liquid-solid adsorption system, some of the features of the adsorbate influencing the adsorption process is the solubility, associated to hydrophobic interactions;

polarity; molecular size, which influences the accessibility to the pores of activated carbon; if the adsorbate has aromatic substituents, which may affect the interactions of dispersion between the adsorbate aromatic rings and, for instance, the graphene layers of the carbon, due to the retention or release of electrons; and further, the pK_a in the case of dealing with an electrolyte because it determines the degree of dissociation. The latter parameter is, in turn, associated with the pH of the solution which may also influence the adsorption capacity, as the ionic strength of the solution and the adsorbate concentration (Bond, 1967; Dabrowski et al., 2005; Moreno-Castilla, 2004; Nabais et al., 2008).

The main characteristics of the adsorbent which affect the adsorption capacity are the porous structure, the functional groups or atoms at the surface (surface chemistry of the carbon) and the content in mineral matter (ash content). Also, the surface area is a factor which influences the adsorption capacity of the adsorbent since the adsorbate will concentrate on the surface of the adsorbent (Bond, 1967; Dabrowski et al., 2005; Moreno-Castilla, 2004; Nabais et al., 2008; Pereira, 2012).

1.4. STUDY BACKGROUND

As it was mentioned above, the pharmaceutical compounds are part of the called emerging pollutants, being more and more necessary to find techniques that are, at the same time, low cost and effective. Activated carbons show several properties that are suitable for application in treatment processes, however, are yet expensive materials. So, the use of industrial residues for the production of activated carbon is a subject which raised attention in the last years, continuing however to be explored. Contrary, the study of removal of fluoxetine from aqueous media is not often found in literature despite the large number of publications mentioning its presence in the environment (Calisto, 2011). That way, the general purpose of this study was the production of three chemically activated carbons with potassium hydroxide (PS800-10KOH), sodium hydroxide (PS800-10NaOH) and zinc chloride (PS800-10$ZnCl_2$), using paper mill primary sludge (PS) as a starting material, and to test their capacity to adsorb fluoxetine. The use of this residue for production of carbon makes it a material of added value, once, beyond the fact of using an industrial residue, it is also renewable resource as it comes from the biomass.

1.4.1. Main goal of the study

The main goal of this study was, as mentioned before, the production of three activated carbons from primary paper mill sludge and to test their adsorptive capacity for fluoxetine-HCl. The results will be compared with those obtained using a carbon produced from the primary sludge pyrolysed without activation (PS800-10) and with a reference commercial activated carbon (PBFG4). For that, kinetics and equilibrium studies were performed using a batch experimental approach. The pyrolysis conditions were the same for all the produced carbons (maximum temperature of 800°C, residence time of 10 minutes, heating ramp of 10°C/min and under nitrogen atmosphere) as well as the impregnation ratio of precursor/activating agent (1:1 w/w).

The produced carbons material were also characterized by different characterization techniques, namely, Fourier transform infrared spectroscopy with attenuated total reflectance (FTIR-ATR), Total organic carbon (TOC), Proximate and Ultimate Analysis, BET surface area and Hg porosimetry, and Scanning electron microscopy (SEM). Also, the PZC of the different carbons were determined using batch experimental approach. Also the spectra of ^{13}C-NMR solid state for PS and PS800-10 are presented. These performed previously in other studies (Calisto et al., 2014).

Experimental data obtained from the batch experiments for kinetic and adsorption equilibrium were fitted to the models described in literature in order to evaluate the adsorption capacity of the produced carbons and also to try to understand the adsorption mechanism of fluoxetine-HCl on these materials.

2. MATERIALS AND METHODS

2.1. CHEMICALS

Fluoxetine-HCl (>98%) was purchased from TCI Europe. For the chemical activation the chemicals were: potassium hydroxide (99.5 %, Fluka), sodium hydroxide (99.3%, José Manuel Gomes dos Santos, Portugal) and zinc chloride (98 %, Riedel-de Haën).

For capillary electrophoresis a 20mM sodium tetraborate (Riedel-de Haën) buffer solution was used as background electrolyte and 0.1M sodium hydroxide (99.3%, José Manuel Gomes dos Santos, Portugal).

For the determination of zero point charge 1.0M HCl (37%, Panreac), 1.0M sodium hydroxide (99.3 %, José Manuel Gomes dos Santos, Portugal) and 0.1M sodium chloride (≥ 99.5 %, Fluka) solutions were prepared.

All solutions were prepared using ultra-pure water, obtained from a Milli-Q Millipore system (Milli-Q plus 185).

2.2. PREPARATION OF ACTIVATED CARBONS

2.2.1. Impregnation and pyrolysis conditions and washing step

For the production of the activated carbons primary sludge (PS) from paper mill industry was used as precursor. This sludge is obtained from a mill kraft pulp with a elemental chlorine free production process, which uses, as raw material, eucalyptus wood (*Eucalyptus globulus*). PS was dried at room temperature in an oven at 60ºC for 24 h and then it was grinded with a blade mill (Calisto et al., 2014).

The chemical agents used for activation were potassium hydroxide, sodium hydroxide and zinc chloride in the ratio 1:1 (w/w). For the preparation of each carbon about 60 g of primary sludge was weighted and impregnated with approximately 60 g of the chemical agent dissolved in 480 mL of ultra-pure water, except for the one impregnated with KOH where 30 g of primary sludge and 30 g of chemical agent were used and the later was dissolved in 240 mL of ultra-pure water (Table 4).

Table 4 – Weighted masses of starting material and of activating agent for the chemical activation

Activating agent	Mass of activating agent / g	Mass of PS / g
KOH	30.0010 ± 0.0001	30.2909 ± 0.0001
NaOH	60.0179 ± 0.0001	60.1431 ± 0.0001
$ZnCl_2$	60.4044 ± 0.0001	60.0433 ± 0.0001

The impregnated materials were placed in polypropylene tubes and agitated at 80 rpm for 24 hours at 25.0 ± 0.1 ºC and dried for 48 hours in a weak air stream atmosphere. The activated sludge were then placed in porcelain crucibles for pyrolysis which was carried out under inert environment (nitrogen flow) at 800ºC with a heating rate of

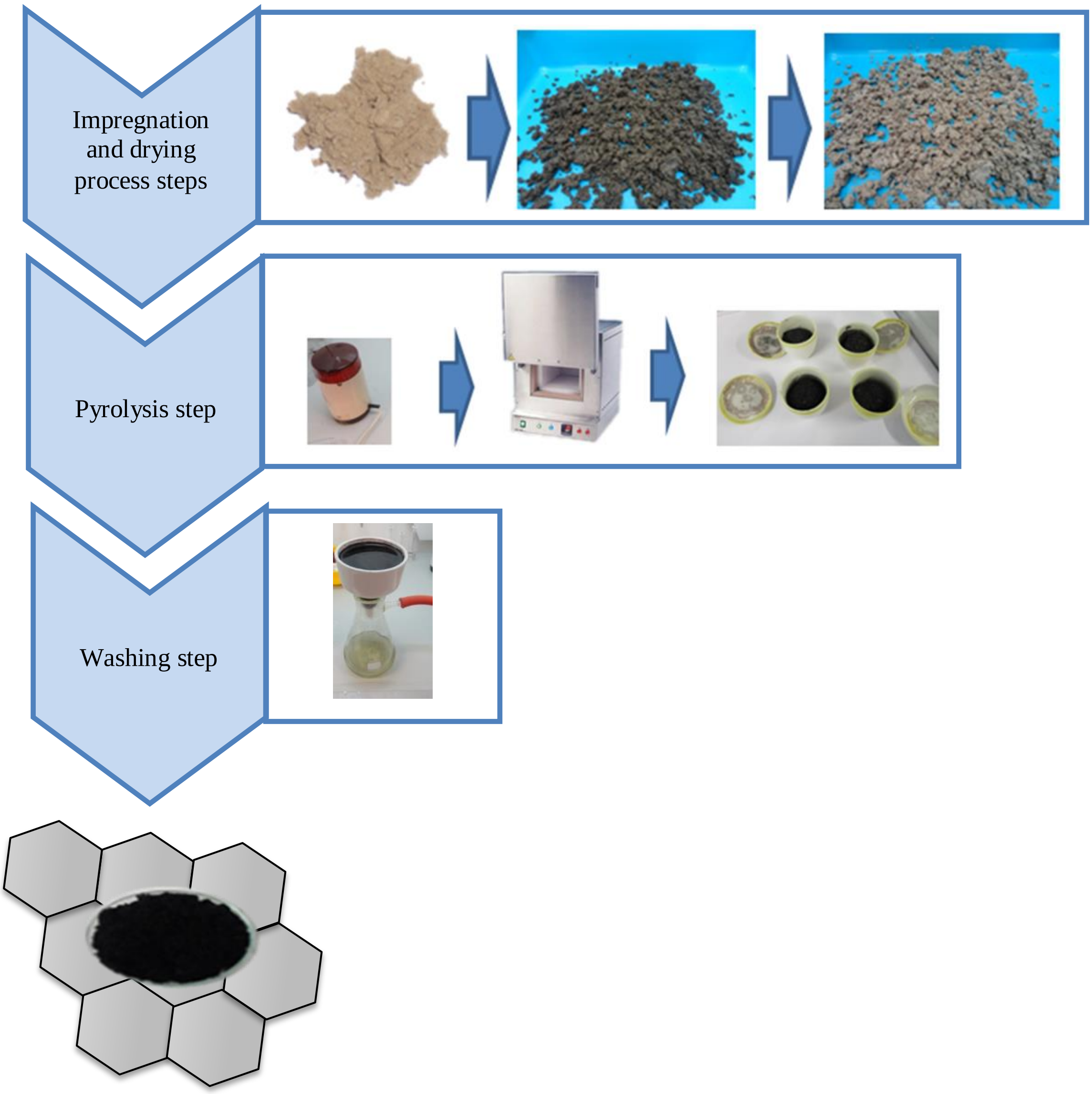

Figure 8 – Process of production of activated carbons

10ºC min^{-1} and with 10 minutes of residence time. After pyrolysis, the hydroxide activated carbons were washed with distilled water until neutral pH and the carbon activated with zinc chloride was washed with 500 mL of HCl 1.2 M followed by distilled water neutral pH (Figure 8). The washing procedures were adapted from Hayashi et al. (2000) and Khalili et al. (2000), respectively. Subsequently, the samples were dried in an oven at 105ºC for 24 hours and crushed mechanically. According to the preparation conditions, the produced activated carbons were named as PS800-10KOH, PS800-10NaOH and PS800-10$ZnCl_2$, corresponding to primary sludge pyrolysed at 800 ºC for 10 minutes impregnated with KOH, NaOH and $ZnCl_2$, respectively. The same pyrolysis conditions were also applied to the primary sludge without activation and the resultant char was named PS800-10. After testing these carbon materials and in order to study the influence of carbonates on the adsorption process, the carbons activated with KOH and NaOH were washed with a solution of HCl 1.0 M followed by distilled water. These carbons were named as PS800-10KOH-HCl and PS800-10NaOH-HCl.

2.3. CHARACTERIZATION OF THE ACTIVATED CARBON

2.3.1. Fourier transform infrared spectroscopy with attenuated total (FTIR-ATR)

The characterization of the carbons included the qualitative analysis of the carbon functional groups. The FTIR-ATR (Fourier transform infrared spectroscopy with attenuated total reflectance) spectra were obtained through a Shimadzu-IRaffinity-1, using an attenuated total reflectance (ATR) module, with a nitrogen purge. The measurements were recorded in the range of 600-4000 cm^{-1}, 4.0 of resolution, 128 scans and with atmosphere and background correction.

2.3.2. TOC

Total organic carbon (TOC) was calculated by difference between the total carbon (TC) content and inorganic carbon (IC) content, that were determined through a TOC analyzer (TOC-VCPH Shimadzu, solid sample module SSM-5000A). Firstly, the total organic carbon was calculated. For that, 30 mg of a standard, glucose ($C_6H_{12}O_6$, 40% of carbon), was measured to test the calibration curve, previously made, and then the carbon samples were analyzed. The mass of carbon material used was 30 mg and three replicates of each sample were measured. The same procedure was made for inorganic carbon determination. In this case, the standard used was sodium carbonate (Na_2CO_3), with a carbon percentage of 11%.

2.3.3. Proximate and Ultimate Analysis

For complementing the latter analysis, proximate and ultimate analyses were performed. This analysis was performed in a LECO TGA-601 automatic analyzer. There were employed standard methods to determine the moisture (UNE 32002), volatile matter (UNE 32019) and ash content (UNE 32004). The fixed carbon was determined as the remaining fraction after ash and volatile matter (at dry basis) determination (Calisto et al., 2014). Ultimate analysis were performed in a LECO CHNS.932 analyzer, determining the content in C, H, N, S and O in the samples at both dry and ash free basis. The oxygen content was calculated by difference between 100% and the percentages of C, H, N, S. Elemental contents were all corrected considering moisture content of the samples in order to present them at a dry basis; the contribution of water for the percentage of O and H was also used to correct elemental analysis (Calisto et al., 2014).

2.3.4. BET surface area and Hg porosimetry

Specific surface area (S_{BET}) and Hg porosimetry have been made for the physical characterization of the carbons. The N_2 adsorption isotherm at -196ºC was analyzed on a Micromeritics ASAP2420 apparatus in order to determine BET surface area, total pore volume (V_p), micropore volume (W_0), average micropore width (L) and average pore diameter (D). Micropore volume and average micropore width were determined by the Dubinin-Radushkevich (DR) equation. The apparent density (ρ_{Hg}) was determined by Hg porosimetry in a Micromeritics Autopore IV 9500 mercury porosimeter. These determinations followed normalized procedures, namely, the samples were outgassed overnight at 100ºC under vacuum prior to adsorption measurements and S_{BET} was calculated from the Brunauer–Emmett–Teller equation (Brunauer et al., 1938) in the relative pressure range 0.01–0.1. V_p was estimated from the amount of nitrogen adsorbed at a relative pressure of 0.99 (Calisto et al., 2014).

2.3.5. Scanning electron microscopy (SEM)

Scanning electron microscopy (SEM) images were obtained at different magnitudes using a Hitachi SU-70 in order to observe the superficial morphology of the produced carbons. The magnitudes employed were 500x, 3000x, 10000x and 30000x.

2.4. POINT OF ZERO CHARGE (PZC) DETERMINATION

The point of zero charge of the carbons was determined by batch equilibration. For each carbon, two different masses (corresponding to the highest and lowest concentration of carbon used in the forthcoming fluoxetine-HCl adsorption experiments) were shaken in polypropylene tubes containing 10 mL of 0.1M NaCl at different initial pH (pH_i) in the range between 2 and 11. Initial pH values had been adjusted with NaOH or HCl (0.1 M and 0.01M), keeping a constant ionic strength. For PS800-10 the masses weighted were 8 and 0.25 mg; for PS800-10KOH 8 and 0.15 mg; for PS800-10NaOH 7 and 0.5 mg; for PS800-10$ZnCl_2$ 3.5 and 1 mg, for PBFG4 1.4 and 0.4 mg. After shaking during 360 minutes for PS800-10, PS800-10KOH, PS800-10NaOH and PBFG4 and 420 minutes for PS800-10$ZnCl_2$ at temperature of 25ºC, the final pH was measured. The point of zero charge was also determined for PS800-10NaOH-HCl. The masses weighted were 4 and 0.5 mg and the carbon was shacked with the solutions of different pH for 180 minutes at 25ºC and the final pH was measured. Then, the PZC was determined by plotting the ΔpH (pH_f-pH_i) versus pH_i, the PZC corresponding to the pH value where the curve crosses the x-axis (Prola et al., 2013). The choice of making the measurements with two masses of carbon is to verify if there was a significant variance in the PZC values between the lower and highest concentration of carbons.

2.5. BATCH ADSORPTION EXPERIMENTS

2.5.1. Kinetics experiments

Kinetic studies were performed to determine the equilibrium adsorption time. For this purpose 10 mg L^{-1} fluoxetine-HCl aqueous solutions were shaken between 5 and 480 minutes with a specific amount of adsorbent. The times used for this determination were 5, 10, 30, 60, 120, 240, 360 and 480 minutes.

Preliminary test preceded these experiments in order to assure that there were no carbon matrix effects and no adsorption of fluoxetine-HCl to the polypropylene tubes and also to determine the ratio between the amount of carbon and the volume of fluoxetine-HCl solution. In order to test matrix effects, a defined amount of carbon was shaken with ultra-pure water and, after filtration, the supernatant and the supernatant spiked with a known concentration of fluoxetine-HCl were analysed by CZE. For testing the possibility of adsorption of fluoxetine-HCl to the polypropylene tubes, the pharmaceutical solution was shaken without the presence of the adsorbent, analyzed by CZE and compared with the result obtained with the same solution prior to contact with the polypropylene tubes. In all batch experiments, samples were filtrated with 0.22 µm PVDF Millipore membranes (Millex-GV).

The masses were measured in a microbalance with an uncertainty of ± 0.001 mg. The volumes of fluoxetine solutions were measured with a 1-10 mL mLine single channel pipette from BioHit. In all kinetic studies 10 mg L^{-1} fluoxetine-HCl solutions were prepared in volumetric flasks.

For the PS800-10, PS800-10KOH and PS800-10NaOH carbons, the mass ratio of adsorbent was 0.075 grams of carbon per liter of solution. Thus, for these 1.5 mg of carbon was weighted and added to 20 mL of fluoxetine solution. For PBFG4, the mass ratio used was 0.04 g L^{-1}, so 0.8 mg of carbon was added to 20 mL of solution. In the case of PS800-10$ZnCl_2$ and PS800-10NaOH-HCl the mass ratio required was 0.2 g L^{-1}, thus 2 mg of these carbons were weighted and added to 10 mL of solution. The solutions were placed in

45mL or 15 mL polypropylene tubes. All the experiments were performed in triplicate and carried out in an overhead shaker (Heidolph, Reax 2) at 80 rpm under controlled temperature (25ºC). In each experiment the pharmaceutical solution was also shaken without the presence of the adsorbent as control testing. The solutions were then filtrated and analysed by CZE in order to determine the remaining concentration of fluoxetine-HCl. The adsorbed amount of fluoxetine-HCl at time *t*, q_t ($mg.g^{-1}$) was calculated by (equation 1).

Two kinetic models, *pseudo-first* order and *pseudo-second* order, were used to analyse the experimental data of fluoxetine-HCl adsorption. Least-squares regression method was used to fit these models to the experimental data.

The experimental data were treated using MatLab 7.0 software for the integration of the peaks and GraphPad (Prism 5) software for the nonlinear regression fit.

2.5.2. Adsorption equilibrium experiments

The procedure used for equilibrium experiments was identical to that described to kinetics experiments. The mass ratio used for kinetic experiments were selected in order to result in 50% of adsorption of fluoxetine. According to that, other mass ratios were selected in order to try to cover the range between 0 and 10 mg L^{-1} of fluoxetine in solution after equilibrium.

Therefore, 10 mL or 20 mL of 10 mg L^{-1} fluoxetine-HCl solution were shaken for a specific time (according to the time needed to attain the equilibrium, determined in the kinetics experiments) in polypropylene tubes of 15 or 45 mL, respectively, with different amounts of the adsorbent. For the carbons PS800-10, PS800-10KOH and PS800-10NaOH the concentration range was 0.025 g L^{-1} to 0.900 g L^{-1}, 0.030 g L^{-1} to 0.140 g L^{-1} for PBFG4 and 0.100 g L^{-1} to 0.400 g L^{-1} for PS800-10$ZnCl_2$.

The concentration of fluoxetine-HCl in equilibrium was determined by CZE (according to section 2.6.2) and calculated using equation (1), for equilibrium studies.

All the experiments were performed in triplicate and carried out in an overhead shaker (Heidolph, Reax 2) at 80 rpm under controlled temperature (25ºC). In each experiment the pharmaceutical solution was also shaken without the presence of the adsorbent as control testing. The adsorbed amount of fluoxetine-HCl at equilibrium, q_e (mg g^{-1}) was calculated by (equation 1).

The models used to fit the experimental data were the ones described in 1.3.2., namely Langmuir, Freundlich, Sips, Redlich-Peterson, Hill, Zhu-Gu and MBET isotherms. Least-squares regression method was used to fit these models to the experimental data.

The experimental data were treated using MatLab 7.0 software for the integration of the peaks and GraphPad (Prism 5) software for the nonlinear regression fit.

2.5.3. Statistical evaluation of the kinetic and isotherm parameters

The kinetic and isotherm parameters were initially evaluated by the correlation coefficient, R^2; however, this parameters is not sufficient to select the best model because as it just gives information about the fit of the points to the model. The correlation coefficient is given by the software GraphPad (Prism 5) and is calculated by the equation 11.

$$R^2 = 1 - \frac{SS_{regression}}{SS_{total}} \qquad \text{(equation 11)}$$

$SS_{regression}$ is the sum of squares of the regression and SS_{total} is the total sum of squares. Therefore, other parameters were tested, namely the Akaike Information Criterion (*AIC*) and the Marquardt's Percent Standard Deviation (*MPSD*) or $F_{\mathrm{error}(\%)}$ (Foo and Hameed, 2010; Hadi et al., 2010). These parameters are calculated using the equations 12 and 13 (Foo and Hameed, 2010; Hadi et al., 2010).

$$AIC = 2p + n\,ln\left(\frac{SS_{res}}{n}\right) \qquad \text{(equation 12)}$$

$$MPSD = 100 \times \sqrt{\left(\frac{1}{n-p}\right)\sum_{i=1}^{n}\left(\frac{q_{e,\,exp} - q_{e,\,model}}{q_{e,\,exp}}\right)^2} \qquad \text{(equation 13)}$$

being p the number of estimated parameters included in the model; n, the sample size; SS_{res}, the residual sum of squares; $q_{e,model}$ the value of q predicted by the fitted model and $q_{e,exp}$, value of q measured experimentally.

The *AIC* criterion is a methodology that takes in account the number of parameters of the model, choosing the model that best fit the experimental data with the minimum number of parameters. The most adequate model is the one with the lowest AIC value (Hadi et al., 2010).

MPSD is used to test the adequacy and accuracy of the model fit with the experimental data and takes in account the number of degrees of freedom of the data. It is an error function used to minimize the error distribution between the experimental equilibrium data and predicted isotherms (Foo and Hameed, 2010; Kumar et al., 2008).

2.6. QUANTIFICATION OF FLUOXETINE-HCl BY CAPILLARY ZONE ELECTROPHORESIS

For the quantification of fluoxetine-HCl, CZE was applied using a Beckman P/ACE MDQ (Fullerton, CA, USA) system equipped with a UV/VIS detector and controlled by the software 32 Karat.

The separation was made using a bare fused silica capillary (40 cm x 75 µm i.d.).

2.6.1. Optimization of the Quantitative Method of Analysis and Operating Conditions

For the optimization of the quantitative method of analysis three main methods were tested (table 5). These three methods were modified in order to verify which conditions were the best for the quantitative analysis. The first method, identified in the Table 5 as **1_Coated capillary column**, was based in the micellar electrokinetic chromatography (MEKC), using a sodium borate electrolyte (buffer) together with sodium dodecyl sulfate (surfactant agent). In this method, the samples contained an internal standard (IS) (ethyl vanillin at 3.4 mg L^{-1}), because once the sample injection is made by pressure, it cannot be ensured that the amount of sample that enters the capillary is reproducible. Thus, the use of internal standard minimizes the uncertainties associated with the injection volume. However, in this case, despite this method has an acceptable response it does not always presented repeatability, it failed during the calibration step, and a calibration curve with an acceptable coefficient of correlation was not achieved. Subsequently, it was decided to alter the conditions of the analysis, testing other methods with non-coated capillary column, namely, **2_Non-coated capillary column (buffer: phosphoric acid)** and **3_Non-coated capillary column (buffer: sodium borate.** These methods were based in capillary zone electrophoresis (CZE). The chosen method is the one with the operating conditions presented in the last row of Table 5, are presented the selected parameters for which were obtained good repeatability.

Table 5 – Results of the variation of some parameters of analysis for method optimization

Parameters	*Experimental conditions*	**Quality Control**
1_Coated capillary column Conditioning and coating step (20 psi): NaOH 1M (30 min); H_2O (15 min); polybrene (20 min); H_2O (2 min); buffer (20min)		
Capillary column washing	Before start the analysis: buffer (20 min) At the end of the analysis: H_2O (7 min)	Area ratio* RSD% = 3.9 (n=3)
Buffer	25 mM sodium borate and 50 mM SDS	
Sample	1500 µL of fluoxetine-HCl solution (5 mg L^{-1}) + 30 µL IS	
Potential supply / kV	25	
Temperature /ºC	25	
Wavelength /nm	200	
Capillary column washing	Before start the analysis: buffer (20 min) At the end of the analysis: H_2O (7 min)	Area ratio RSD% = 6.7 (n=3)
Buffer	25 mM Borate and 50 mM SDS	
Sample	1350 µL of fluoxetine-HCl solution (5 mg L^{-1}) + 30 µL IS + 150 µL de sodium borate 25 mM	
Potential supply / kV	25	
Temperature /ºC	25	
Wavelength /nm	200	
Capillary column washing	Before start the analysis: buffer (20 min) At the end of the analysis: H_2O (7 min)	Area ratio RSD% = 15.4 (n=3)
Buffer	25 mM sodium borate and 40 mM SDS	
Sample	1500 µL de fluoxetine-HCl solution (5 mg L^{-1}) + 30 µL IS	
Potential supply / kV	25	
Temperature /ºC	25	
Wavelength /nm	200	
Capillary column	Before start the analysis: buffer (20 min)	Area ratio

washing	At the end of the analysis: H_2O (7 min)	RSD% = 3.7
Buffer	25 mM sodium borate and 20 mM SDS	(n = 3)
Sample	1500 µL fluoxetine-HCl solution (5 mg L^{-1}) + 30 µL IS	
Potential supply / kV	25	
Temperature /ºC	25	
Wavelength /nm	200	
Capillary column washing	Before start the analysis: buffer (20 min) At the end of the analysis: H_2O (7 min)	
Buffer	20 mM Borato e 40 mM SDS	Area ratio
Sample	1500 µL fluoxetine-HCl solution (5 mg L^{-1}) + 30 µL IS	RSD% = 9.2 (n=15)
Potential supply / kV	25	
Temperature /ºC	25	
Wavelength /nm	200	
Capillary column washing	Before start the analysis: buffer (20 min) At the end of the analysis: H_2O (7 min)	
Buffer	25 mM Borato e 20 mM SDS	Area ratio
Sample	1500 µL fluoxetine-HCl solution (5 mg L^{-1}) + 30 µL IS	RSD% = 7.4 (n=6)
Potential supply / kV	25	
Temperature /ºC	25	
Wavelength /nm	220	
2_Non-coated capillary column (buffer: phosphoric acid)		
Capillary column washing	Before start the analysis: buffer (20 min) At the end of the analysis: H_2O (7 min)	No peak detection during 30 min of separation
Buffer	20 mM H_3PO_4	
Sample	1500 µL fluoxetine-HCl solution (10 mg L^{-1})	
Potential supply / kV	25	
Temperature /ºC	25	
Wavelength /nm	200	
3_Non-coated capillary column (buffer: sodium borate) Conditioning step (20 psi): NaOH 1M (15 min); H_2O (2min); Sodium Borate Buffer (3 min)		
Capillary column washing	Before start the analysis: buffer (20 min) At the end of the analysis: H_2O (7 min) Intermediate wash step at each 6 runnings with: 0,1 M NaOH (5 min) followed by ultra-pure water (2 min)	Peak area RSD% =3.4% (n=12)
Buffer	40 mM sodium borate	

Sample	1500 µL fluoxetine-HCl solution (10 mg L^{-1})	
Potential supply / kV	25	
Temperature /ºC	25	
Wavelenght /nm	200	
Capillary column washing	**Before start the analysis: buffer (20 min)** **At the end of the analysis: H_2O (7 min)** **Intermediate wash step at each 12 runnings with: 0,1 M NaOH (5 min) followed by ultra-pure water (2 min)**	**Peak area RSD% =1.7% (n =12)**
Buffer	**20 mM sodium borate**	
Sample	**1500 µL fluoxetine-HCl solution (10 mg L^{-1})**	
Potential supply / kV	**25**	
Temperature /ºC	**25**	
Wavelength /nm	**200**	

*Area ratio = Peak area of fluoxetine-HCl/Peak area of IS

Therefore, the chosen operating conditions (according with the results in Table 5) are presented next.

The capillary was conditioned before its first use by flushing 1.0 M NaOH for 10 minutes, then with water for 5 minutes and finally with the electrolyte solution for 2 minutes.

The separation conditions for quantification of fluoxetine-HCl were as follows:

- Rinse the capillary with electrolyte 20mM of sodium borate for 2 min at 20psi
- Inject sample by hydrodynamic injection for 4 s at 0.5 psi
- Inject separation buffer 20mM of sodium borate for 3 s at 0.5 psi
- Separate with separation buffer 20mM of sodium borate for 2 minutes at 25KV, 25ºC, recorded at 200 nm.

Every 12 sample injections the capillary was rinsed with 0.1M NaOH for 5 minutes and water for 2 minutes for strengthening the capillary wall charge. The electropherogram is presented in Figure 9.

Separate vials of electrolytes were used for rising and separating operations in order to keep the electrolyte level constant during separation. Triplicate injections of solutions were performed and the average peak areas were used for quantification.

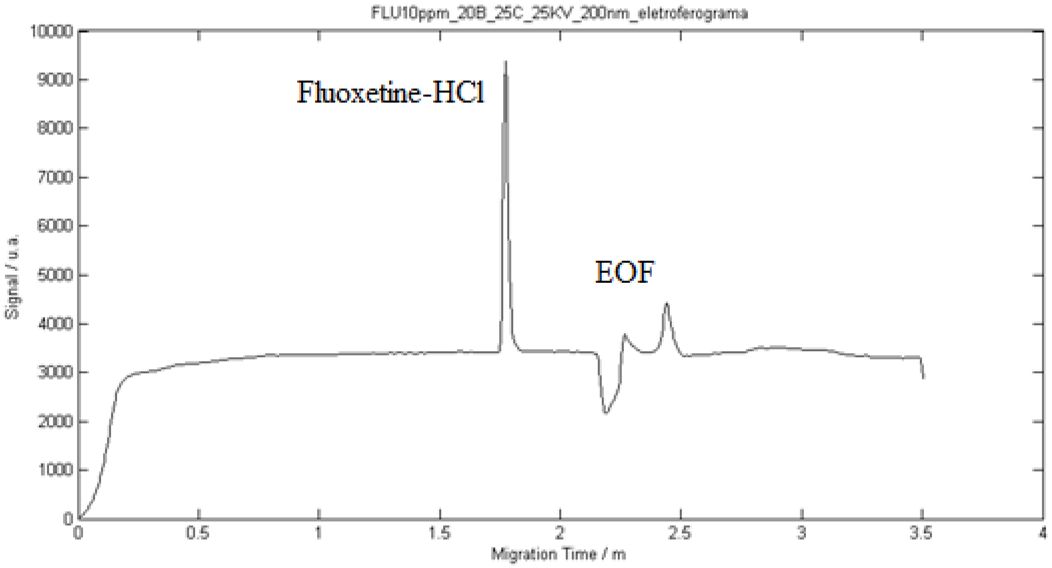

Figure 9 – Electropherogram of a 10 mg L^{-1} fluoxetine-HCl solution (EOF – electroosmotic flow)

Fluoxetine peak appears before the electroosmotic flow which means that the molecule is in it protonated form, since pK_a of fluoxetine is 9.5 and the buffer has a pH of 9.

The detection wavelength was chosen according to the UV-Vis absorption spectrum (Figure 10) of fluoxetine-HCl, which was obtained with a UV-Vis spectrometer T90+ PGInstruments Ltd.).

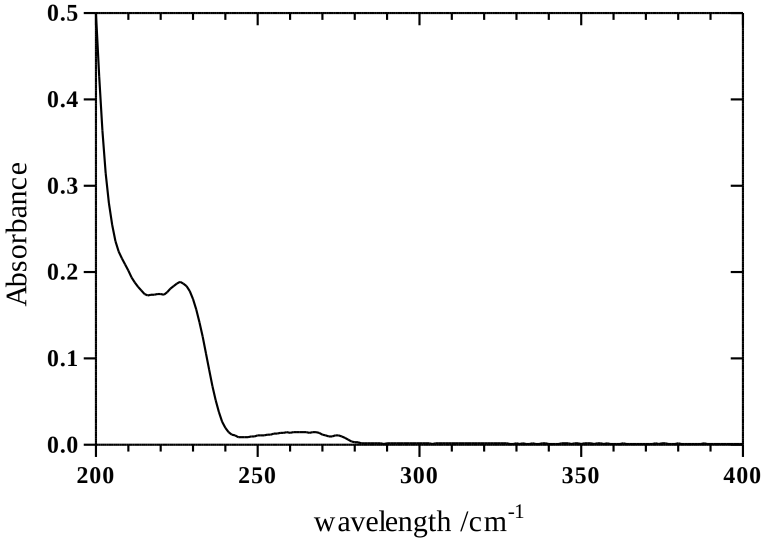

Figure 10 – Fluoxetine-HCl absorption spectrum

Analysing the spectrum we can observe that fluoxetine present a well-defined peak at 226 nm and another zone, around 200 nm, in which there has an exponential increase of absorption. The precision tests were made using the wavelength of 200 nm and, although this value is in a zone of accentuated slope, this fact do not influenced the repeatability of the results.

2.6.3. Calibration curve

The quantification of fluoxetine-HCl was made using a calibration curve with standard between 0.50 and 10.00 mg L^{-1}.

After the optimization step, it was determined the calibration curve using seven standard solutions of fluoxetine-HCl of 0.5, 1.0, 2.0, 4.0, 6.0, 8.0, 10.0 mg L^{-1}, prepared by dilution of a 100 mg L^{-1} stock solution using 10 mL volumetric flasks. Three replicates of each standard solution were performed and the correlation coefficient for the calibration curve was above 0.995. After that, the samples were analyzed. A linear calibration curve was obtained for each new capillary, using the least-squares linear regression method. The correlation coefficients range 0.9974 to 0.9983.

The equation of the regression curve is given by

$$y = a + bx \qquad \text{(equation 14)}$$

were y is the peak area, x is the concentration of the solution, b is the slope of the curve and a is the intercept on the y-axis (Miller and Miller, 2010).

One of the calibration curve obtained is presented in figure 16 (section 3.2.1.).

The errors in the slope, s_b, and intercept, s_a, of the regression were calculated by:

$$s_b = \frac{s_{y/x}}{\sqrt{\sum_i (x_i - \bar{x})^2}} \qquad \text{(equation 15)}$$

$$s_a = s_{y/x}\sqrt{\frac{\sum_i x_i^2}{n\sum_i (x_i - \bar{x})^2}} \qquad \text{(equation 16)}$$

where $s_{y/x}$ is a estimative of the random errors in the y-direction, calculated by equation (17):

$$s_{y/x} = \sqrt{\frac{\sum_i (y_i - \hat{y}_i)^2}{n-2}} \qquad \text{(equation 17)}$$

The limit of detection (LOD) and the limit of quantification (LOQ) were calculated according to:

$$\textit{limit of detection (LOD)} = \boldsymbol{y_a + 3s_a} \qquad \text{(equation 18)}$$

$$\textit{limit of quantification (LOQ)} = \boldsymbol{y_a + 10s_a} \qquad \text{(equation 19)}$$

where y_a is the value of the intercept, which can be considered as the blank signal of the method and s_a is the standard deviation of the intercept (Miller and Miller, 2010).

Also, the precision or repeatability of the method was calculated when integrating the peak areas. The precision describes the random error, evaluating the dispersion of the response for a set of replicates and is analyzed calculating the coefficient of variation (CV) or relative standard deviation (RSD) (equation 20) (Miller and Miller, 2010).

$$\boldsymbol{RSD}\ (\%) = \boldsymbol{100\frac{s}{\bar{x}}} \qquad \text{(equation 20)}$$

Where s and $\bar{\boldsymbol{x}}$ are the standard deviation and the average, respectively, of the obtained values.

3. RESULTS AND DISCUSSION

3.1. CHARACTERISATION OF THE CARBONS

After the production of the activated carbon the production yield was calculated. The yield obtained for the produced carbons were 64% for PS800-10, 24% for PS800-10KOH, 28% for PS800-10NaOH and 26% for PS800-10ZnCl$_2$. It is observed differences between the value for the non-activated carbon (PS800-10) and the values obtained for the activated carbons. Part of this difference can be attributed to the washing step in which there are inevitably losses of material, and on the other hand it can also be due to a higher decomposition due to the reaction with the activating agents.

3.1.1. FTIR-ATR analysis

The FTIR-ATR analysis were performed to identify the structure of the carbon materials, namely, the surface composition which is important to recognize and understand the adsorption process, once great part of the adsorption process is due to the functional groups that can be present in the carbon surface.

The FTIR-ATR spectra of the carbons are represented in Figure 11.

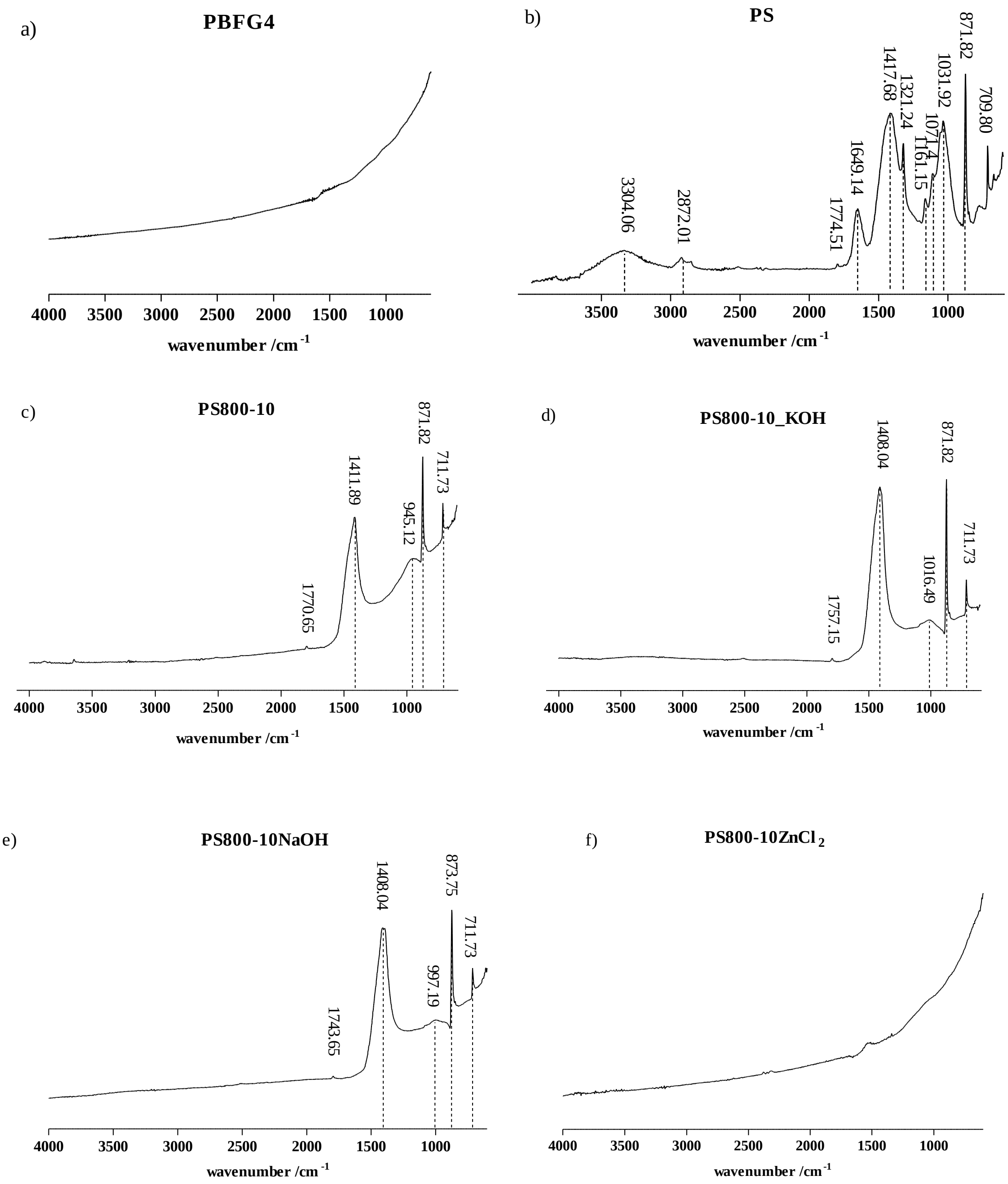

Figure 11 – FTIR-ATR spectra (Abs versus Wavenumber) for the carbons a) PBFG4, b) PS, c) PS800-10, d) PS800-10KOH, e) PS800-10NaOH and f) PS800-10ZnCl$_2$.

By the general overview of all spectra it can be seen that the precursor (PS) has a more complex chemical composition than the pyrolysed materials. PS has several bands that disappear after pyrolysis and activation, namely around 3300 cm^{-1} and 2872 cm^{-1}

corresponding to a —OH phenol or alcohol groups (Ahmad et al., 2007; Bansal and Goyal, 2005; Devi and Saroha, 2013; Hassan et al., 2014; Maas, 1972) and to C—H stretch vibrations due to interaction with the carbon surface (Ahmad et al., 2007; Coates, 2000; Maas, 1972), respectively. With respect to the *fingerprint* region it can be observed the presence of two bands characteristic of carbonate ion, namely, the bands around 1410 and 870 cm^{-1} (Coates, 2000; Maas, 1972). The presence of other peaks are also observed such as at 1031 cm^{-1}, 1071 cm^{-1} and 1161 cm^{-1} that can be attributed to C—O—C stretching vibration of pyranose ring (skeletal) (Yang et al., 2007). The peak at 1321 cm^{-1} can be related with C—H bending vibrations (Yang et al., 2007) and the peaks in the range 750-450 cm^{-1} are recognized as in-plane and out-plane aromatic ring deformation vibrations, C—H and C—C stretching (Devi and Saroha, 2013; Yang et al., 2007). The peaks at 1649 and 1774 cm^{-1} can be related to C═C benzene stretching ring (Coates, 2000; Yang et al., 2007). The referred bands present in spectrum of PS are typical of cellulosic materials, mainly in the region of functional groups (Sevilla and Fuertes, 2009; Yang et al., 2007).

The spectra of PS800-10, PS800-10KOH and PS800-10NaOH are very similar between each other presenting bands around the same wavenumbers varying only in intensity and in the *fingerprint* region. In these spectra, as observed in the PS spectrum, it can be observed the presence of the two bands characteristic of carbonate ion (Coates, 2000). The other peaks observed are at 711 cm^{-1}, possibly related to in-plane and out-plane aromatic ring deformation vibrations, C—H and C—C stretching (Devi and Saroha, 2013; Yang et al., 2007), between 940 and 1020 cm^{-1} attributed to cyclohexane derivatives (Maas, 1972) and a slight peak around 1760 that can be due to C═C benzene stretching ring (also present in PS) (Coates, 2000; Yang et al., 2007).

The FTIR-ATR spectrum of PS800-10ZnCl$_2$ present only a small peak at around 1500 cm^{-1} characteristic of aromatic compounds due to aromatic ring vibrations (aromatic carbon-carbon stretching vibrations) (Coates, 2000) being very similar to the spectrum of the reference activated carbon. Is important to refer that the structure of activated carbons is mainly aromatic, consisting in layers of carbon, similar to polynuclear aromatic molecules (Bandosz, 2006; Marsh and Rodríguez-Reinoso, 2006; McElroy, 2005).

3.1.2. ^{13}C-NMR study

As mentioned in 1.4.1. ^{13}C-NMR solid state was previously performed (Figure 12 a) and b)).

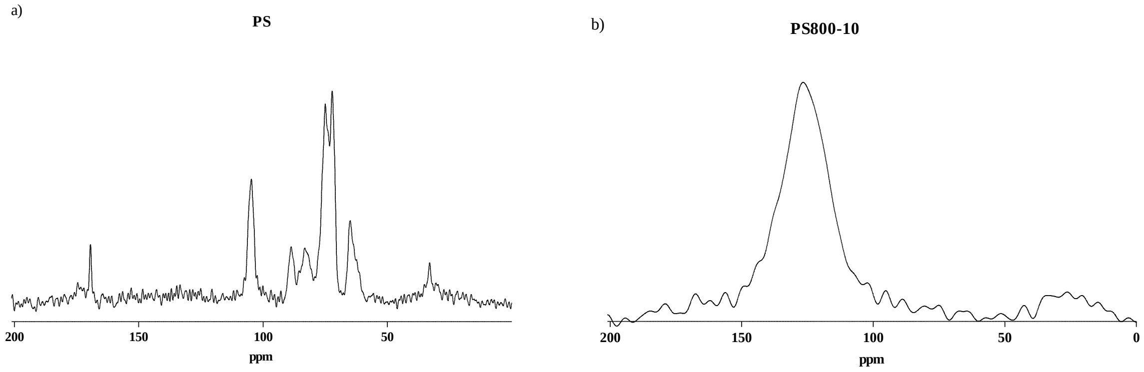

Figure 12 – ^{13}C-NMR solid state spectra for PS (a) and PS800-10 (b)

The PS spectrum is similar to the cellulose spectrum, showing four main regions related with the cellulose carbons (Figure 13), namely, C1 at 105 ppm; C4 at 89 and 83 ppm; C2,3,and 5 at 75 and 72 ppm and C6 at 65 ppm (Calisto et al., 2014; Kobayashi et al., 2011; Larsson et al., 1999). Also, in the aromatic region, between 110 and 160 ppm, it present no peaks.

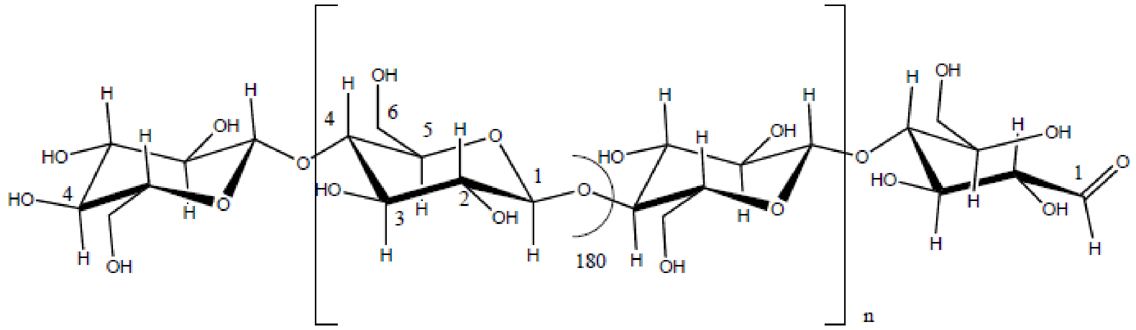

Figure 13 - Molecular structure of cellulose (Granström, 2009)

The main difference between the spectra are that the PS800-10 spectrum present mainly a wide peak between 110 and 160 ppm, corresponding to aromatic functional groups (Figure 12 b) (Burrows and Pereira, 2006; Calisto et al., 2014). It is known that cellulose pyrolysed under inert atmosphere gives rise to graphite-like structures due to a mechanism of thermal degradation which includes the dehydration of the cellulosic chain

(Tang and Bacon, 1964). Therefore, the pyrolysis leaded to the disappearing of the cellulose structure and to the formation of aromatic structures proving to be adequate to the production of carbon materials. The results obtained by ^{13}C NMR are consistent with the ones obtained for FTIR-ATR analysed in the previous section (3.1.1.).

3.1.3. Total Organic Carbon

The results of the total organic carbon for the materials under study are present in table 6.

It can be seen in table 6 that only PS800-10ZnCl$_2$ achieved a larger percentage of total carbon content, very similar to the commercial activated carbon. In carbons PS800-10KOH and PS800-10NaOH this percentage is lower than in PS, the difference being in the percentages of organic carbon that are the smallest of all the materials. The percentage of inorganic carbon in PS, PS800-10, PS800-10KOH and PS800-10NaOH can be related to the presence of carbonates in these materials according to FTIR-ATR spectrums, which are not present in PS800-10ZnCl$_2$ due to the acid washing step.

Table 6 – Total Organic Carbon (TOC) analysis for PS and the pyrolysed materials (n=3).

Carbon material	TC (%) Mean ± SD	IC (%) Mean ± SD	OC (%) Mean ± SD
PS	33.0 ± 0.8	8.84 ± 0.05	24.1 ± 0.9
PBFG4	77.5 ± 0.1	0.04 ± 0.04	77.4 ± 0.2
PS800-10	33.7 ± 0.3	4.7 ± 0.4	29.0 ± 0.6
PS800-10KOH	23.4 ± 0.1	8.1 ± 0.2	15.3 ± 0.2
PS800-10NaOH	27.2 ± 0.1	7.8 ± 0.3	19.4 ± 0.3
PS800-10ZnCl$_2$	72.4 ± 0.4	—	72.4 ± 0.4

TC – Total Carbon; IC – Inorganic Carbon; and OC – Organic Carbon

3.1.3. Proximate and ultimate analysis

Proximate and ultimate analysis results are presented in Table 7. PS800-10$ZnCl_2$ show characteristics closer of that one of commercial activated carbons once it is the only one that has low ash content and the highest carbon content. According to Yu et al. (2013), the ash content of a conventional activated carbon should not exceed the 10%. It is also visible a decrease in hydrogen content, related to the aromatization of the carbon structure (Pietrzak et al., 2013).

The results of TOC analysis are consistent with the ones of proximate and ultimate analysis. It can also be seen that the ratio between volatile matter and fixed carbon (VM/FC) is lower for PS800-10$ZnCl_2$ (Table 7) which might be related to a higher evolution of volatile matter in this carbon.

Also, in PS800-10, PS800-10KOH and PS800-10NaOH there exist a high percentage in oxygen which can influence the adsorption capacity. The oxygen content can be in the form of ─OH or C═O groups which affect the surface chemistry of the carbons.

Table 7 ─ Proximate and Ultimate Analysis results for PS, PS800-10, PS800-10KOH, PS800-10NaOH and PS800-10$ZnCl_2$

	Proximate Analysis (wt.%, db)					***Ultimate Analysis (wt.%, db)***				
SAMPLE	***Moisture content (wt.%)***	Ash	Volatile Matter (VM)	Fixed Carbon (FC)	VM/FC	C	H	N	S	O
PS	1.57	55.31	36.09	8.60	4.20	14.83	1.26	0.40	0.29	27.91
PS800-10	3.15	50.50	31.40	18.10	1.73	28.81	0.47	0.33	0.60	19.29
PS800-10KOH	3.02	52.03	35.66	12.31	2.90	21.30	0.48	0.24	0.14	25.81
PS800-10NaOH	1.70	47.90	32.68	19.42	1.68	25.95	0.54	0.28	0.04	25.29
PS800-10$ZnCl_2$	3.72	14.30	10.10	75.60	0.13	77.36	0.90	0.59	0.96	5.89

% O = 100% - (Ash+C+H+N+S)%; *db:* dry basis

3.1.5. Specific surface area and porosity

Results from the textural characterization of the carbons here considered are shown in Table 8.

Among the produced materials from PS, PS800-10ZnCl$_2$ is the one that presents the highest BET surface area being in the same order of magnitude of the reference carbon (PBFG4) and being between 300 and 4000 m^{2}g^{-1}, which is characteristic of the activated carbons (Yang, 2003). Also, the micropore volume is about 67% of the total pore volume. Zinc chloride is known as an activating agent that increases the microporosity development, however its utilization is quite limited due to environmental considerations (Bandosz, 2006; Radovic, 2008). Another aspect that can be noticed is the fact that PS800-10KOH has a larger surface area than the one activated with NaOH although the fixed carbon in PS800-10KOH is less than in PS800-10NaOH, suggesting a better carbonization of the latter. PS800-10NaOH has the same total pore volume than the PS800-10 and about half of the micropore volume, which explains why the BET surface area of that carbon is half of the one of PS800-10. The same analysis can be made with PS800-10KOH and the pyrolysed sludge. The decrease in micropore volume of these two carbons and the difference in carbon content between them can be related to the destruction of the microporous structure resulting from the extreme conditions of the activation which is done by impregnation (Pietrzak et al., 2013) and moreover because of the presence of the ashes, that can occlude the micropores. Apparent density is defined as the mass of unit volume of the carbon particle, including its pore system (Marsh and Rodríguez-Reinoso, 2006). The carbon that present a lower value of apparent density is PS800-10ZnCl$_2$, from that it can be inferred, again, that this carbon has a relative high porosity.

Table 8 – Textural parameters of the carbons: S_{BET} – BET surface area; V_p – total pore volume; W_o – micropore volume; L – average micropore width; D – average pore diameter.

Sample	**Apparent density, ρ_{Hg} (g cm^{-3})**	**N_2 adsorption at −196 °C**				
		S_{BET} (m^2 g^{-1})	**V_p (cm^3 g^{-1})**	**Dubinin-Radushkevich (DR)**		**D (nm)**
				W_0 (cm^3 g^{-1})	**L (nm)**	
PBFG4	0.55	848.22	0.36	0.295	1.30	0.84
PS800-10	0.515	120.86	0.0850	0.0469	0.88	1.41
PS800-10KOH	0.50	114.71	0.10	0.05	1.27	1.74
PS800-10NaOH	0.52	60.45	0.08	0.02	1.72	2.74
PS800-10$ZnCl_2$	0.39	591.92	0.33	0.22	1.28	1.10

3.1.6. SEM analysis

The SEM analyses (Figure 14) were performed to observe the external morphology of the carbons. In figure 14a) it is seen the intact fibrous nature of the raw material. This surface is slightly modified with the pyrolysis (PS800-10 figure 14 b)). In Figures 14 c), d) and e), the surface appearance is rougher. However, in PS800-10$ZnCl_2$ it is seen some degree of destruction of the fibers but not so accentuated as in PS800-10KOH and PS800-10NaOH. In PS800-10KOH and PS800-10NaOH the external surfaces are sponge like and quite irregular appearing to have some cavities. These cavities could be created due to the aggressive attack of the reagent during the activation and evaporation of the chemical agent (KOH and NaOH, respectively) during the pyrolysis (Sirimuangjinda et al., 2013), and therefore they correspond to the porosity. They can also be result from the release of volatiles (Khalil et al., 2013). However, during the activation process, inorganic residues are produced and might not be effectively removed in the washing step. Therefore, the general appearance of PS800-10KOH and PS800-10NaOH may be due to small particles of inorganic residues present in these two carbons (Sirimuangjinda et al., 2013). In PS800-10$ZnCl_2$ the degree of destruction seems to lower, nevertheless, it is clearly observed some real cavities in the material.

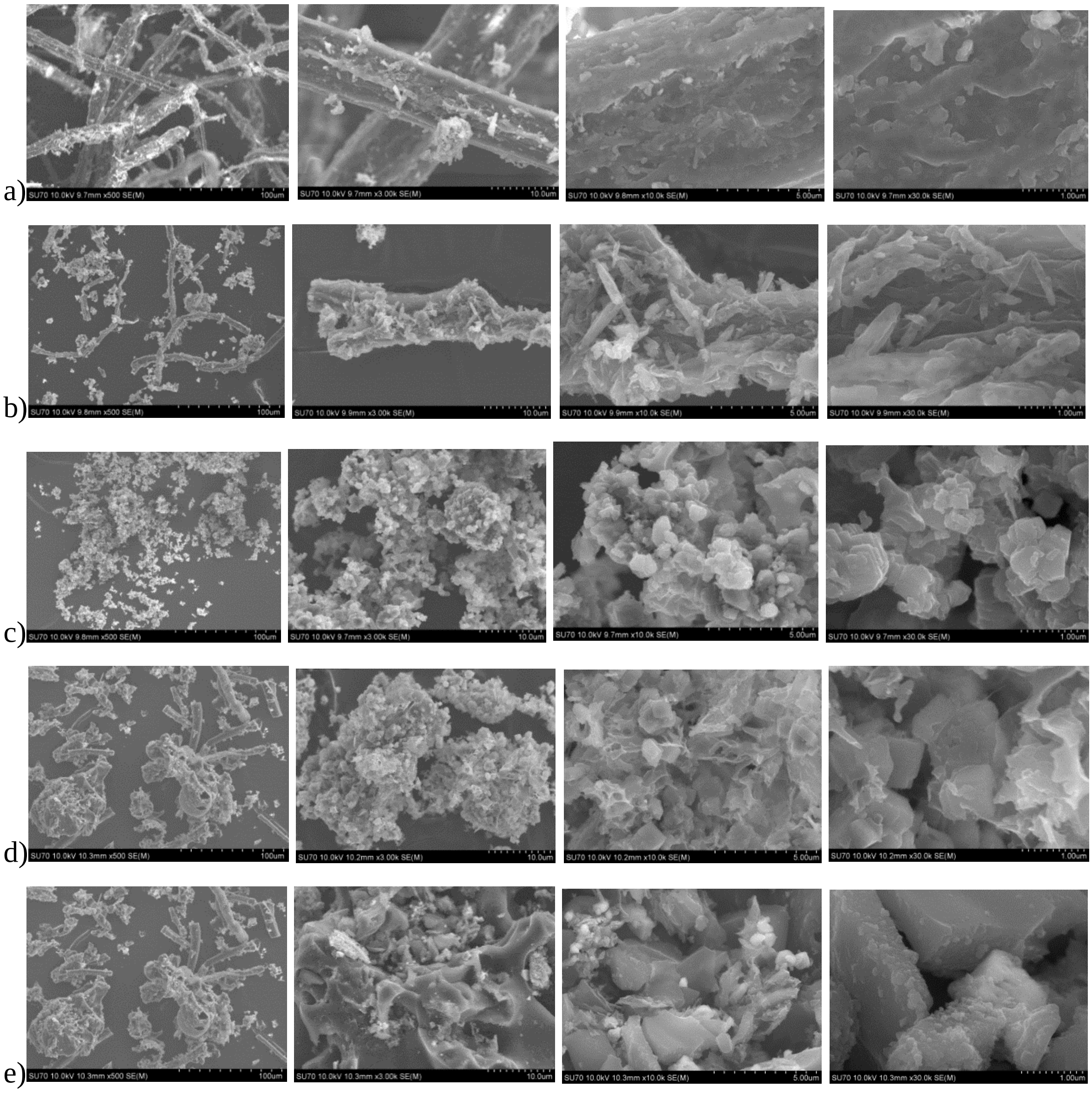

Figure 14 – Scanning electron microscopy images of a) PS; b) PS800-10; c) PS800-10KOH; d) PS800-10NaOH; e) PS800-10ZnCl$_2$ at 500x, 3000x, 10000x and 30000x (from left to right).

3.1.7. Point of zero charge (PZC) determination

The determination of PZC allows to determine the acidity or basicity of the carbon material which influences the pH of the solution and the possible electrostatic interactions between adsorbate and adsorbent (Petrova et al., 2010). In figure 15 a), b), c), d) and e) it can be seen the plots obtained of ΔpH vs pH_i which allow to see how the carbon behaves at different pH.

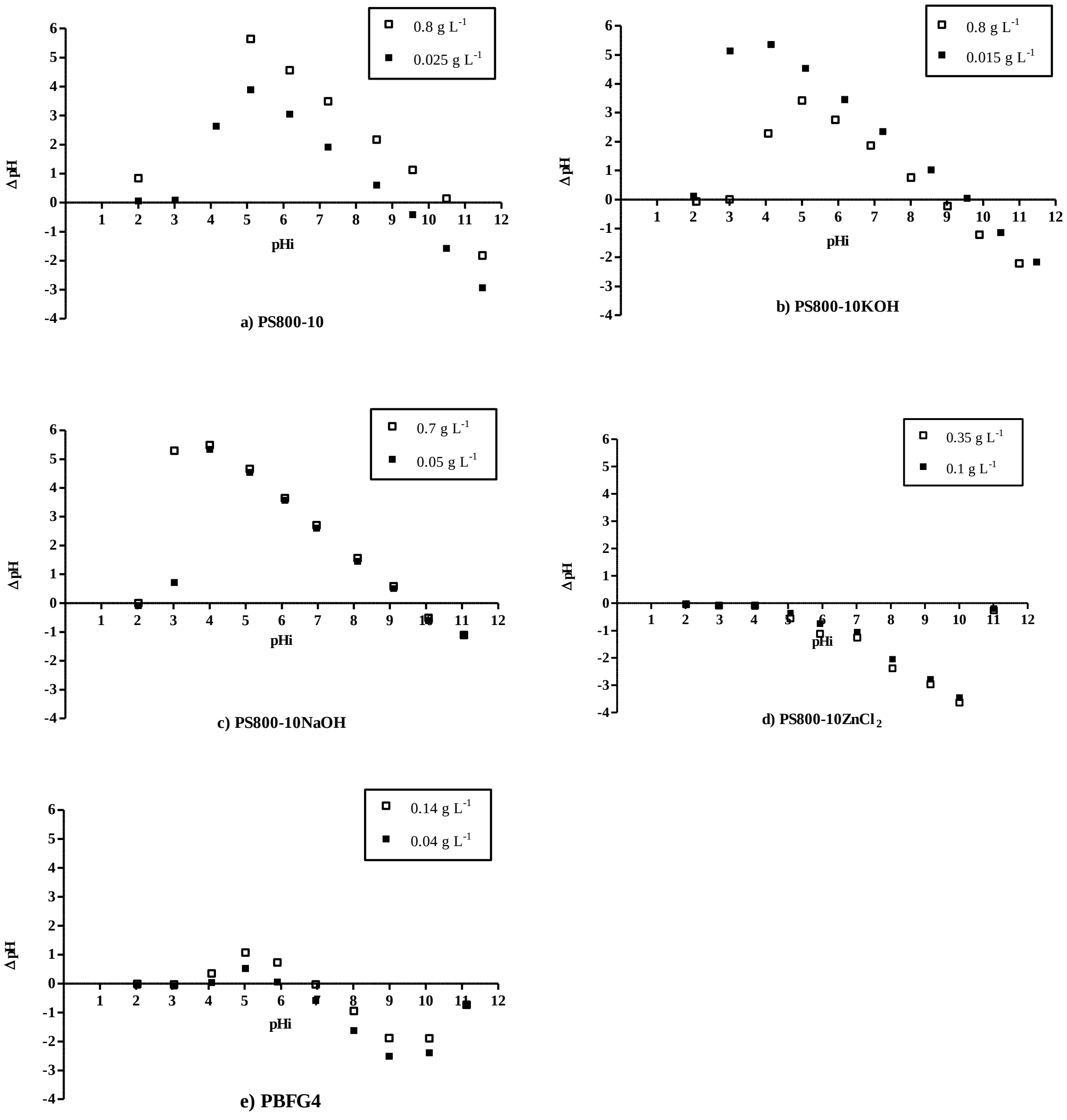

Figure 15 – Plots of ΔpH *vs* pH_i for the determination of PZC.

PS800-10ZnCl$_2$ and PBFG4 have PZC values below pH 7, namely, around 4-5 and 6-7, respectively. PS800-10, PS800-10KOH and PS800-10NaOH, present PZC values above pH 7 and very close to the pK_a value of fluoxetine (9.5) (Nabais et al., 2008). By control experiments performed (tests of carbon in water and carbon in 10 mg L^{-1} fluoxetine-HCl solution) it was concluded that the pH of the fluoxetine-HCl solutions in contact with the carbon is equal to its PZC, which is, consequently, the working pH for the adsorption studies, once the solutions were not buffered for the adsorption tests. From these results it can be said that for PS800-10$ZnCl_2$ and PBFG4, who PZC is below 9.5, fluoxetine-HCl mainly is in the protonated form, having a positive charge. Meanwhile, for PS800-10, PS800-10KOH and PS800-10NaOH, whose PZC is around 9.5, the cationic and the neutral forms of fluoxetine-HCl are both present in the same ratio. Also, since the solutions acquire a pH value similar to the PZC of the carbons, these present a net charge of zero during the experiments.

3.2. ADSORPTION STUDIES – KINETICS AND EQUILIBRIUM ADSORPTION

3.2.1. Calibration curve results

As mentioned in 2.6.3., a calibration curve was obtained for each new capillary used. An example of one of those calibration curves is presented in Figure 16.

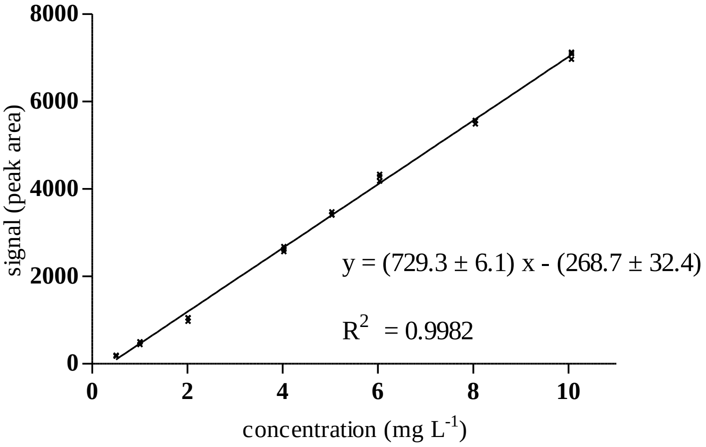

Figure 16 – Calibration curve for the determination of fluoxetine solutions concentrations.

The values of LOD and LOQ obtained were 0.151 mg L^{-1} and 0.502 mg L^{-1}, respectively. In this work the peak areas responses presented an RSD% less than 15% and the migration times less than 2%, which are good values once no IS were used in the method.

3.2.2. Experimental adsorption data fitting

The kinetic experiments allowed determining the time necessary for the fluoxetine-HCl solution to achieve the equilibrium in the interface between the bulk solution and the carbon surface. The equilibrium time is an important parameter in the industrial practice once the adsorbents have to possess a good adsorption capacity but also they must adsorb in a useful time. Hence, the equilibrium time was evaluated by plotting the quantity adsorbed versus the respective time of stirring.

As already mentioned, isotherm study allow to determine the maximum capacity of the adsorbent material, in this case, for a specific compound, and also to have an idea, together with the kinetic analysis, of the mechanism of adsorption involved in the process.

Next, kinetic and adsorption fit results for the experimental data obtained for I) PBFG4 reference carbon, II) PS800-10, III) PS800-10KOH, IV) PS800-10NaOH and V) PS800-10ZnCl$_2$ are presented.

I) PBFG4 reference carbon

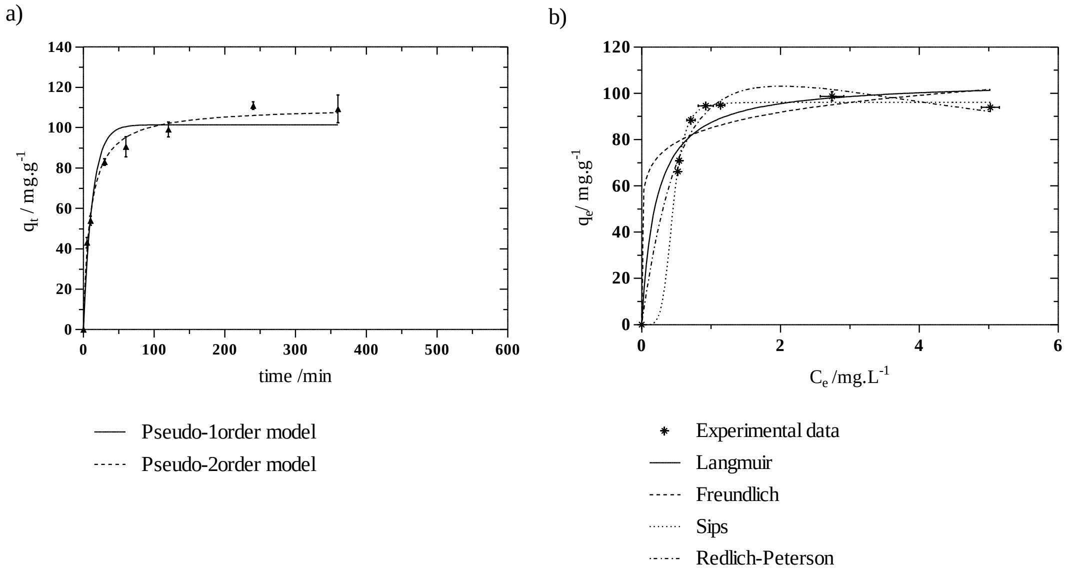

Figure 17 –Nonlinear fit of (a) Pseudo-first order, pseudo-second order kinetic models (for 0.04 g L^{-1} of carbon) and (b) Langmuir, Freundlich, Sips and Redlich-Peterson isotherms model for the reference carbon PBFG4 experimental data (360 min).

Table 9 – Kinetic and Isotherm parameters for the adsorption experimental data of PBFG4 (reference carbon) for fluoxetine-HCl.

Model		Parameters			Fit				
					n	R^2	SS_{res}	*MPSD*	*AIC*
Kinetic model	*PFO*	q_e 101.50 ± 4.22	k_1 0.08 ± 0.01		8	0.9508	437.4	12.51	44.01
	PSO	q_e 110.3 ± 2.5	k_2 0.0009 ± 0.0001			0.9914	90.1	6.14	31.37
Isotherm model	*Langmuir*	q_m 105.5 ± 6.7	K_L 4.82 ± 1.70		8	0.9580	319.10	1.53	41.5
	Freundlich	K_F 85.1 ± 3.7	*n* 9.04 ± 4.00			0.9293	536.9	1.53	45.6
	Sips	q_m 96.2 ± 1.0	K_S 74.14 ± 40.23	*m* 0.19 ± 0.03		0.9983	12.62	1.68	25.0
	Redlich-Peterson	K_{RP} 200.5 ± 27	α_{RP} -1.14 ± 0.32	β 1.34±0.10		0.9894	80.63	25.0	39.8

q_e (mg g^{-1}); q_m (mg g^{-1}); k_1 (min^{-1}); k_2 (g mg^{-1} min^{-1}); K_L (L mg^{-1}); K_F (mg$^{1-1/n}$ L$^{1/n}$ g^{-1}); K_S (L g^{-1}); K_{RP} (L g^{-1}); α_{RP}(L mg^{-1});

II) PS800-10 carbon

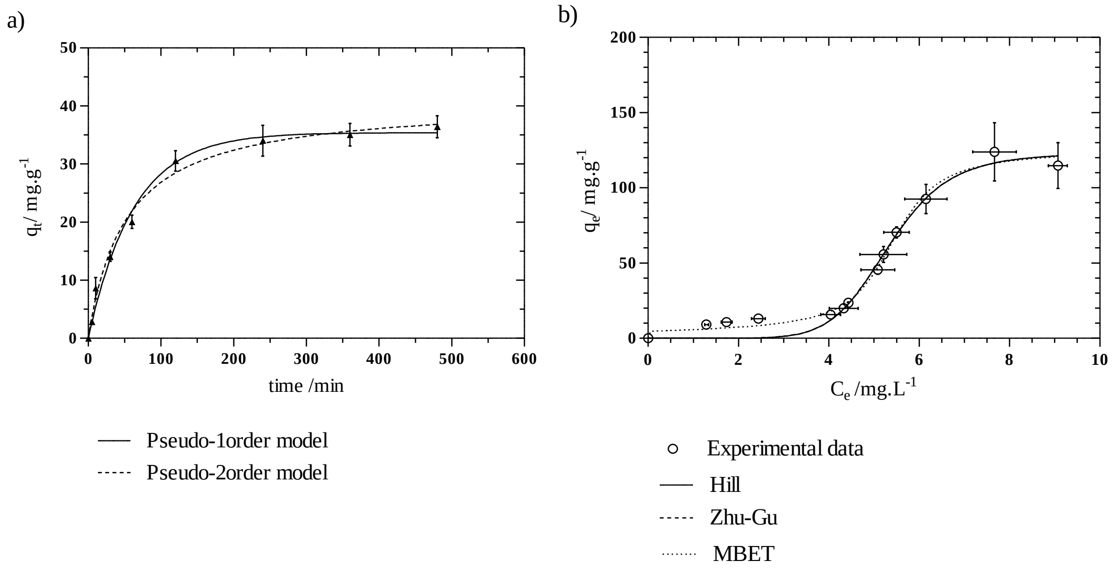

Figure 18 – Nonlinear fit of (a) Pseudo-first order, pseudo-second order kinetic models (for 0.075 g L^{-1} of carbon) and (b) Hill, Zhu-Gu and Modified BET (MBET) isotherms model for the reference carbon P800-10 experimental data (360 min).

Table 10 - Kinetic and Isotherm parameters for the adsorption experimental data of PS800-10 carbon for fluoxetine-HCl.

Model		Parameters				Fit				
						n	*R^2*	*SS_{res}*	*MPSD*	*AIC*
Kinetic model	*PFO*	*q_e* 35.4 ± 0.9	*k_1* 0.016 ± 0.002			9	0.9899	16.83	15.50	16.43
	PSO	*q_e* 40.8 ± 1.4	*k_2* 0.00047±0.00007				0.9917	13.86	13.97	14.69
Isotherm model	*Hill*	*q_m* 122.99 ± 6.39	*K_H* 0.187± 0.004	*b* 7.97 ± 1.22		13	0.9771	493.5	55.03	60.3
	Zhu-Gu	*q_∞* *120*.4 ± 2.5	*K_1* ~	*r* 11.16 ±0.79	*K_2* 3~~,~~.4e-8 ± 3.6e-8		0.9952	103.0	58.01	45.7
	MBET	*q_m* 4.66 ± 0.56	*K_{MBET}* ~	*C_o* 5.45 ± 0.07	*s* 27.41 ± 3.04		0.9918	176.2	21.44	52.5
q_e (mg g^{-1}); *q_m* (mg g^{-1}); *k_1* (min^{-1}); *k_2* (g mg^{-1} min^{-1}); *K_1* and *K_2* (g mg^{-1})										

III) PS800-10KOH carbon

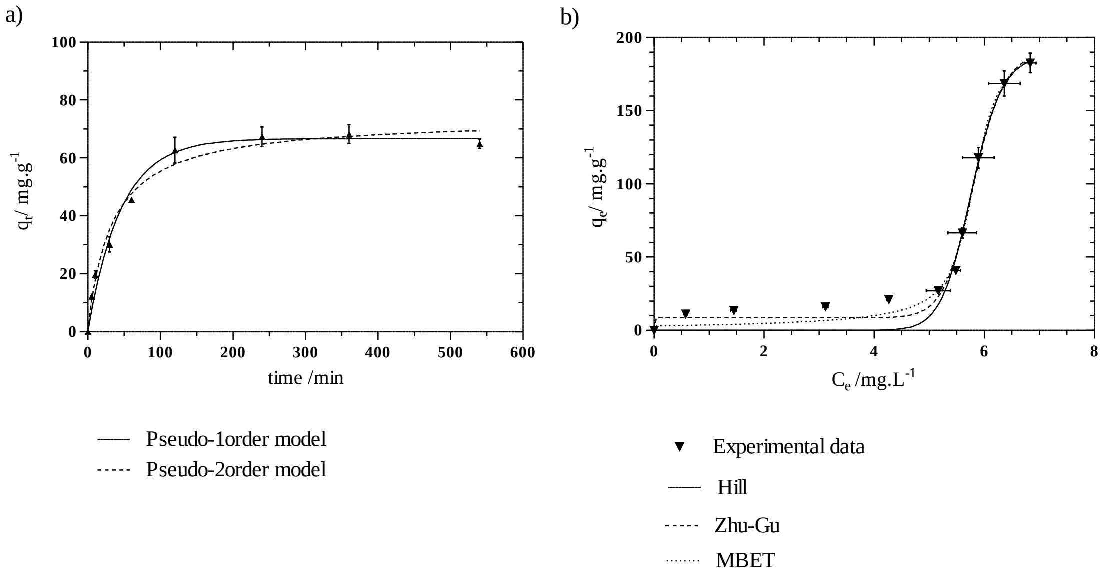

Figure 19 – Nonlinear fit of (a) Pseudo-first order, pseudo-second order kinetic models (for 0.075 g L^{-1} of carbon) and (b) Hill, Zhu-Gu and ModifiedBET (MBET) isotherms model for the reference carbon PS800-10KOH experimental data (360 min).

Table 11 – Kinetic (n=9) and Isotherm (n=11) parameters for the adsorption experimental data of PS800-10KOH carbon for fluoxetine-HCl.

Model		Parameters				Fit				
						n	R^2	SS_{res}	*MPSD*	*AIC*
Kinetic model	*PFO*	q_e 66.7 ± 2.0	k_1 0.022 ± 0.003			9	0.9834	92.73	20.97	48.64
	PSO	q_e 73.6 ± 2.8	k_2 0.00041±0.00008				0.9834	92.55	12.93	41.47
Isotherm model	*Hill*	q_m 189.8±15.02	K_H 0.173 ± 0.002	*b* 20.58±4.75		11	0.9730	1167	71.81	66.0
	Zhu-Gu	q_∞ 191.6 ± 4.8	K_1 ~	*r* 22.03 ±2.48	K_2 8.4e-17 ± 3.7e-16		0.9914	369.7	33.76	60.7
	MBET	q_m 3.1 ±0.6	K_{MBET} ~	C_o 5.82 ±0.08	*s* 64.57 ± 9.47		0.9905	412.3	46.93	61.9

q_e (mg g^{-1}); q_m (mg g^{-1}); k_1 (min^{-1}); k_2 (g mg^{-1} min^{-1}); K_1 and K_2 (g mg^{-1})

IV) PS800-10NaOH carbon

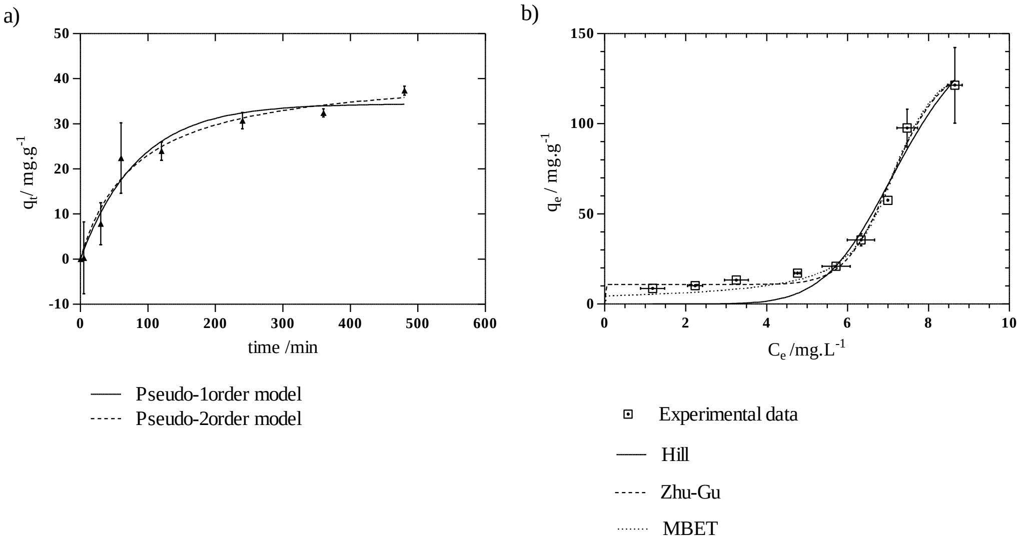

Figure 20 – Nonlinear fit of (a) Pseudo-first order, pseudo-second order kinetic models (for 0.075 g L^{-1} of carbon) and (b) Hill, Zhu-Gu and Modified BET (MBET) isotherms model for the reference carbon PS800-10NaOH experimental data (360).

Table 12 – Kinetic and Isotherm parameters for the adsorption experimental data of PS800-10NaOH carbon for fluoxetine-HCl.

Model		Parameters				Fit				
						n	R^2	SS_{res}	*MPSD*	*AIC*
Kinetic model	*PFO*	q_e 34.5 ± 2.0	k_1 0.012 ± 0.002			8	0.9659	51.99	200.91	26.97
	PSO	q_e 41.9 ± 3.5	k_2 0.0003±0.0001				0.9709	59.94	254.93	25.72
Isotherm model	*Hill*	q_m 159.8 ± 50.3	K_H 0.14 ± 0.01	*b* 7.54 ± 2.84		10	0.9480	710.8	69.76	58.6
	Zhu-Gu	q_∞ 136.6 ± 9.6	K_1 ~	*r* 12.60±1.40	K_2 1.1e-10± 3.0e-10		0.9869	178.5	19.19	53.8
	MBET	q_m 4.55 ± 0.88	K_{MBET} ~	C_o 7.20 ± 0.15	*s* 32.23 ±5.51		0.9870	177.7	28.32	53.8
q_e (mg g^{-1}); q_m (mg g^{-1}); k_1 (min^{-1}); k_2 (g mg^{-1} min^{-1}); K_1 and K_2 (g mg^{-1})										

V) PS800-10ZnCl$_2$ carbon

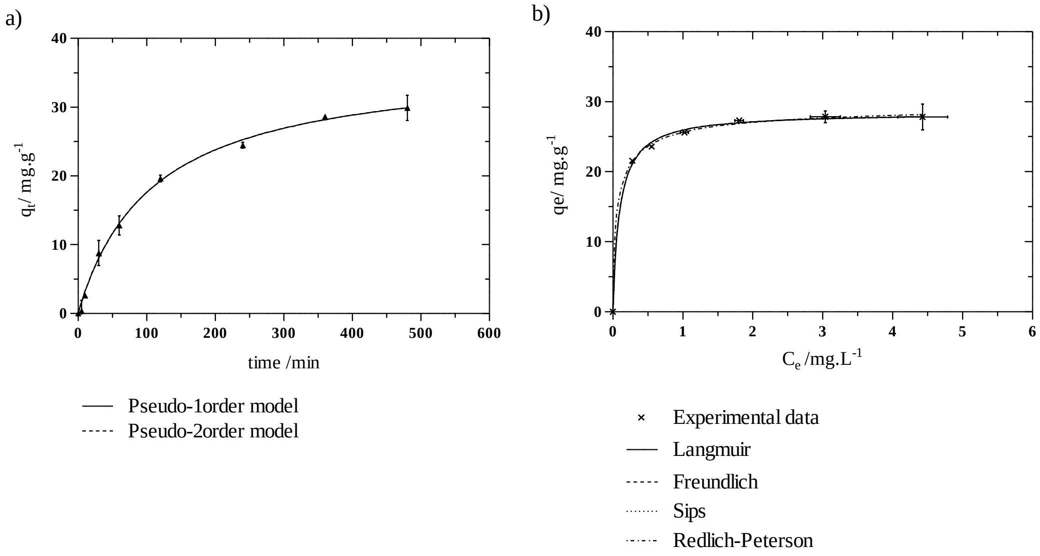

Figure 21 – Nonlinear fit of (a) Pseudo-first order, pseudo-second order kinetic models (for 0.2 g L^{-1} of carbon) and (b) Langmuir, Freundlich, Sips and Redlich-Peterson isotherms model for the reference carbon PS800-10ZnCl$_2$ experimental data (420 min).

Table 13 – Kinetic and Isotherm parameters for the adsorption experimental data of PS800-10ZnCl$_2$ carbon for fluoxetine-HCl.

Model		Parameters			Fit				
					n	R^2	SS_{res}	*MPSD*	*AIC*
Kinetic model	*PFO*	q_e 29.4 ± 0.8	k_1 0.0093 ± 0.0008		9	0.9934	7.59	117.62	9.26
	PSO	q_e 36.67 ± 1.07	k_2 0.00025 ± 0.00003			0.9970	3.489	117.62	2.27
Isotherm model	*Langmuir*	q_m 28.4 ± 0.3	K_L 10.3 ± 1.0		7	0.9984	0.9592	1.83	0.1
	Freundlich	K_F 25.0 ± 0.3	*n* 10.8 ± 1.4			0.9960	2.357	1.83	6.4
	Sips	q_m 29.8 ± 1.2	K_S 6.1 ± 2.0	*m* 1.5 ± 0.4		0.9991	0.5076	2.05	9.6
	Redlich-Peterson	K_{RP} 401.8 ± 116.5	α_{RP} -14.7 ± 4.7	*b* 0.97 ± 0.02		0.9989	0.6505	1.38	11.8

q_e (mg g^{-1}); q_m (mg g^{-1}); k_1 (min^{-1}); k_2 (g mg^{-1} min^{-1}); K_L (L mg^{-1}); K_F (mg$^{1-1/n}$ L$^{1/n}$ g^{-1}); K_S (L g^{-1}); K_{RP} (L g^{-1}); α_{RP}(L mg^{-1})

Initially Langmuir, Freundlich, Sips and Redlich-Peterson models were considered to fit the experimental data. However, for PS800-10, PS800-10KOH and PS800-10NaOH, these models give poor values for the correlation coefficient. Hence, other three models were chosen to fit the data of these carbons, namely, Hill, Zhu-Gu and MBET isotherm models. The choice of the best model for each carbon was done according to the four fitting parameters, R^2, SS_{res}, *MPSD* and *AIC*.

3.2.3. Kinetic studies analysis

The kinetics curves show that the adsorption of fluoxetine-HCl onto carbon materials under study takes around six to seven hours to reach the equilibrium. Moreover, both pseudo-first (PFO) and pseudo-second (PSO) kinetic models fit the experimental data with correlation coefficients (R^2) higher than 0.95. In any case, considering values of error functions (R^2, SS_{res}, *MPSD* and *AIC*), it could be said that the obtained kinetic results are better fitted with the PSO model, which is normally associated to chemical adsorption or chemisorption as the rate-limiting step (Ho and McKay, 1999). Beyond the chemisorption as adsorption mechanism, another assumption can be made for carbons with PSO kinetics, namely, the heterogeneity (chemical or geometrical) of the surface (Ho and McKay, 1999;

Liu, 2008; Marczewski, 2007; Qiu et al., 2009). The chemical heterogeneity of the surface can be related with the heterogeneous surface groups, namely oxygen-containing groups, and inorganic ash, and the geometrical heterogeneity is related to the different pore sizes and shapes and carbon basal planes (Franz et al., 2000; Girods et al., 2009).

3.2.4. Equilibrium adsorption studies analysis

The isotherm shape is an important parameter because it allows diagnosing the adsorption mechanism. The results obtained from the equilibrium adsorption studies and the models fitting isotherms are shown in section 3.2.2. From these, it can be seen that the reference carbon PBFG4 and the produced carbon PS800-10ZnCl$_2$ present a “normal” L type isotherm, with a unique plateau, according to Giles (1960) definition. Meanwhile, the other carbons (PS800-10, PS800-10KOH and PS800-10NaOH) present an S or H type isotherm, which is indicative of cooperative adsorption, showing that the adsorption of fluoxetine-HCl occurs in two consecutive stages.

Equilibrium results on the adsorption of fluoxetine-HCl onto the reference carbon (PBFG4) are fitted to the Sips or Langmuir-Freundlich isotherm model, with a R^2 of 0.9983. This carbon has a maximum adsorption capacity of 96.2 ± 1.0 mg g^{-1} and the low value of m parameter indicates a high surface heterogeneity. This low value is also related to the high surface area of the carbon (Girods et al., 2009). Also the L shape isotherm and PSO fitting of the adsorption kinetics point to a chemisorption mechanism.

For PS800-10ZnCl$_2$ the best adjustment is the one of Langmuir isotherm model with an R^2 of 0.9984 and a maximum adsorption capacity of 28.4 ± 1.2 mg g^{-1}. Langmuir isotherm is related to homogeneous surface of the adsorbent and monolayer adsorption (Foo and Hameed, 2010; Girods et al., 2009). The separation factor, R_L, for this carbon is 0.0096, showing a favorable adsorption (Foo and Hameed, 2010).

$$\boldsymbol{R_L = \frac{1}{1+K_L C_0}} \qquad \text{(equation 21)}$$

Regarding the equilibrium experimental results on the adsorption of fluoxetine-HCl onto PS800-10, PS800-10KOH and PS800-10NaOH, fittings to the Hill isotherm, the Zhu-Gu isotherm and MBET isotherm models were determined. In the case of PS800-10KOH and PS800-10NaOH, the Zhu-Gu model offered the best fitting. The Zhu-Gu isotherm, which is a model capable of describing S-shaped and two-plateau-type isotherms, gave for these carbons a limiting amount adsorbed (second “plateau”) of 191.6 ± 4.8 mg g^{-1} for PS800-10KOH and 136.6 ± 9.6 mg g^{-1} for PS800-10NaOH. This isotherm model describes adsorption process in two stages. During the first one, the solute adsorbs forming a layer on the adsorbent surface as a consequence of surface-solute interactions (first “plateau”, Figure 22). Then, in the second stage, a sharp increase in the adsorption isotherm occurs due to interactions between solute molecules (second “plateau”). Though this was the best fit, the software cannot give values for the affinity parameters, which can be due, according to (Guilarduci et al., 2006), to the heterogeneity of the surface that involves a bigger dispersion in the affinity values leading to a high standard deviation. Also, this dispersion in the affinity may furthermore be related with the fact that the pH of the solution being close to the pK_a value of fluoxetine-HCl, which may have influence in the adsorption mechanism and therefore in the values of the affinity parameters. The limiting amount adsorbed values of PS800-10, PS800-10KOH and PS800-10NaOH are higher than the maximum adsorption capacity of PBFG4 and PS800-10$ZnCl_2$ for fluoxetine-HCl, which could lead to conclude that the former three carbons are better. However, the pH conditions of the solution in PS800-10, PS800-10KOH and PS800-10NaOH were different than in PBFG4 and PS800-10$ZnCl_2$. This difference seems to indicate that a pH close to the pK_a of fluoxetine-HCl benefit their adsorption. So, it remains the question that if the pH of the solution in PBFG4 and PS800-10$ZnCl_2$ adsorption studies were close to the pK_a of fluoxetine-HCl, these carbons would present or not higher adsorption capacity for this compound.

It is also interesting to compare the isotherm of PS800-10$ZnCl_2$ with the first “plateau” obtained for PS800-10, PS800-10KOH and PS800-10NaOH (Figure 22 and Table 14), it can be seen that effectively, the former as a relatively higher adsorption capacity with respect to the “monolayer”, however the other three carbons, that possess much lower surface area than PS800-10$ZnCl_2$, have adsorption capacities in the same order of magnitude of PS800-10$ZnCl_2$. These results lead to another question, put by some authors, related with the importance or not of the specific surface area for the adsorption of some compounds.

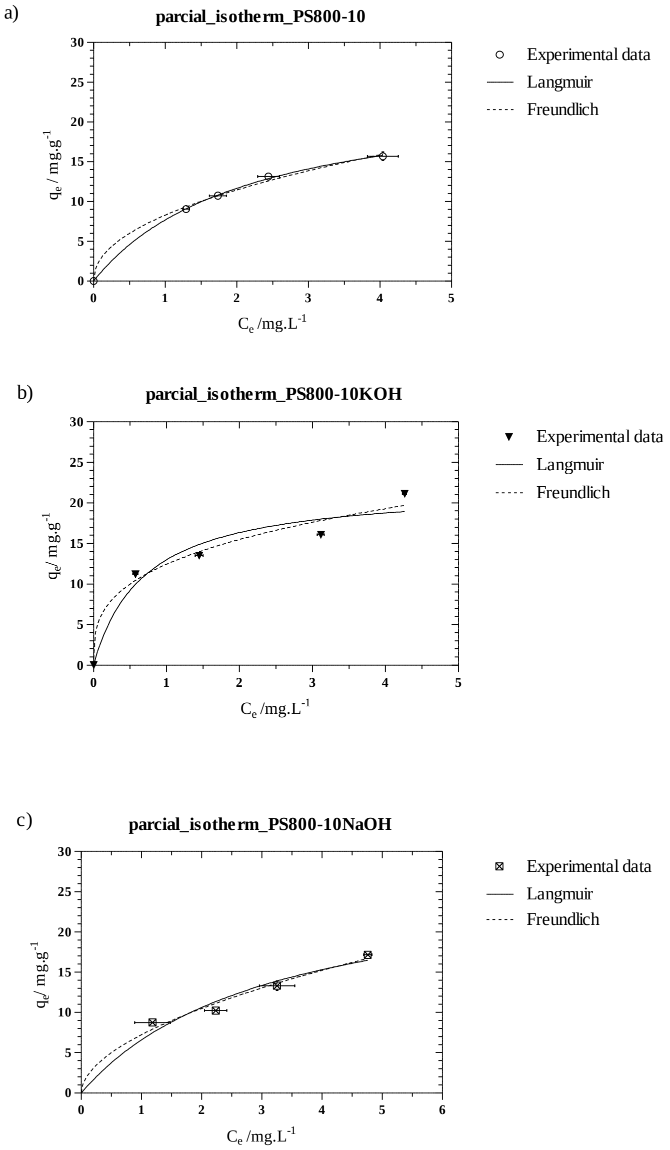

Figure 22 – Magnification of the first “plateau” obtained for the isotherms for PS800-10 (a), PS800-10KOH (b) and PS800-10NaOH (c), with Langmuir and Freundlich isotherm fittings.

Table 14 – Isotherm parameters for the adsorption experimental data of PS800-10, PS800-10KOH and PS800-10NaOH for fluoxetine-HCl at the "first plateau".

Carbon	Isotherm model	Parameters				Fit (n=5)			
						R^2	SS_{res}	*MPSD*	*AIC*
PS800-10	*Langmuir*	q_m	24.2 ± 0.7	K_L	0.47 ± 0.03	0.9994	0.0856	7.51	9.66
	Freundlich	K_F	8.3 ± 0.3	n	2.1 ± 0.2	0.9969	0.4467	19.36	17.9
PS800-10KOH	*Langmuir*	q_m	22.0 ± 2.9	K_L	1.43 ± 0.7	0.9511	12.04	146.73	34.4
	Freundlich	K_F	12.4 ± 1.0	n	3.16 ± 0.7	0.9756	6.010	90.54	30.9
PS800-10NaOH	*Langmuir*	q_m	27.4 ± 5.9	K_L	0.3 ± 0.1	0.9779	3.625	84.9	28.4
	Freundlich	K_F	7.2 ± 0.6	n	1.9 ± 0.2	0.9893	1.745	57.2	24.7
q_e (mg g^{-1}); q_m (mg g^{-1}); K_L (L mg^{-1}); K_F (mg$^{1-1/n}$ L$^{1/n}$ g^{-1})									

Differences between the isotherms of adsorption of fluoxetine-HCl onto the carbons under study may be related with the surface chemical nature (chemical composition and surface functional groups) and with the presence of impurities (Girods et al., 2009; Nevskaia et al., 2001) that affect the pH of the solution. The FTIR-ATR spectra analyzed previously did not show relevant differences between all carbon materials in terms of functional groups. In fact, according to FTIR-ATR and TOC, the main difference between the carbons showing two-plateau isotherms and those showing one-plateau isotherm is the presence of carbonate groups, which have been considered impurities (Nevskaia et al., 2001). The presence of these impurities (carbonates) can influence the PZC values (Nevskaia et al., 2001) of the three carbons PS800-10, PS800-10KOH and PS800-10NaOH, which present 50.50, 52.03 and 47.90 percent of ash content, respectively, and PZC values around 9.5, while PBFG4 and PS800-10ZnCl$_2$ which have very low content in ash present PZC values below 7, namely, 6 and 4, respectively. The PZC values are important in the analysis of the isotherms. In this study, the PZC influence the ionized state of fluoxetine-HCl, since when the carbons are in contact with water, the solution acquires a pH equal to the value of the PZC of the carbons. Once the pK$_a$ of fluoxetine-HCl is 9.5, at pH below the pK$_a$ the compound take mainly the ionized state and at pH equal to the pK$_a$ the ionized and nonionized forms are both present in the same ratio. Furthermore, at high pH values fluoxetine tend to have higher K$_{ow}$ (octanol-water partition coefficient) which means that fluoxetine present higher hydrophobicity (Brooks et al., 2003). These facts can influence the adsorption mechanism, since neutral fluoxetine molecules may interact with each other, which is possible in the case of PS800-10, PS800-10KOH and PS800-10NaOH, possibly justifying the appearance of second plateau in the isotherms. Also, according to Nevskaia et al. (2001), lateral interactions between molecules can be increased by the presence of potassium carbonates. Hence, to verify if the carbonates really influence the appearance of the second plateau present in the isotherms of PS800-10, PS800-10KOH and PS800-10NaOH, the carbon PS800-10NaOH-HCl was tested. This carbon is the same as PS800-10NaOH with the difference that it was washed with an HCl solution as was the carbon PS800-10ZnCl$_2$. This approach allows to conclude that the second plateau of adsorption is due to the presence of carbonates in the carbons. Kinetic and adsorption equilibrium were studied (Figure 24 and Table 15) and characterization studies, namely, FTIR-ATR (Figure 23 a) and PZC (Figure 23 b) were performed.

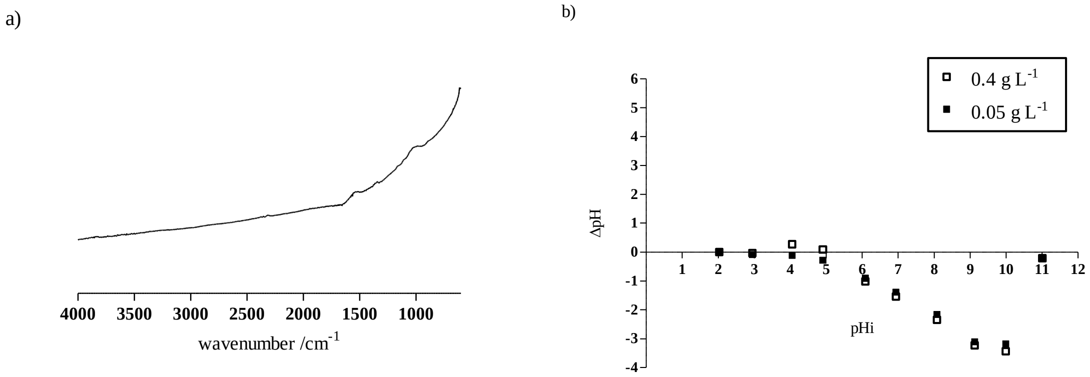

Figure 23 – Characterization study a) FTIR-ATR spectra and b) PZC of PS800-10NaOH washed with HCl (PS800-10NaOH-HCl).

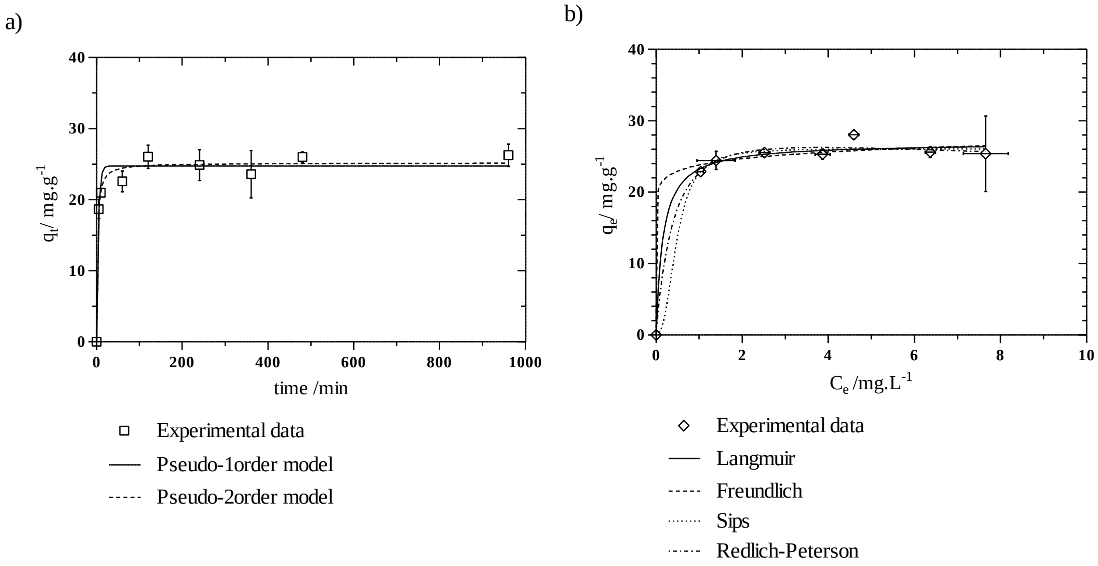

Figure 24 – Nonlinear fit of (a) Pseudo-first order, pseudo-second order kinetic models (for 0.2 g L^{-1} of carbon) and (b) Langmuir, Freundlich, Sips and Redlich-Peterson isotherms model for PS800-10NaOH-HCl experimental data (240 min).

Fittings of the experimental results to the considered kinetic and isotherm models are presented in table 15.

Table 15 – Kinetic and isotherm parameters obtained from various equations to the adsorption data of PS800-10NaOH-HCl carbon material for fluoxetine-HCl.

Model		Parameters			Fit				
					n	R^2	SS_{res}	*MPSD*	*AIC*
Kinetic model	*PFO*	q_e 24.75 ± 0.60	k_1 0.25 ± 0.04		9	0.9712	15.80	6.52	15.86
	PSO	q_e 25.19 ± 0.50	k_2 0.021 ± 0.005			0.9827	9.505	4.86	11.29
Isotherm model	*Langmuir*	q_m 26.91±0.7131	K_L 6.284 ± 2.463		8	0.9894	6.10	3.65	9.83
	Freundlich	K_F 23.80±0.8261	*n* 18.74 ± 8.793			0.9861	8.03	4.00	12.03
	Sips	q_m 26.12±0.6376	K_S 6.411 ± 2.479	*m* 0.3916±0.3842		0.9909	5.22	3.73	17.92
	Redlich-Peterson	K_{RP} 67.82 ± 30.08	α_{RP} -1.994 ± 1.245	*b* 1.113 ± 0.09		0.9920	4.617	3.53	11.37
q_e (mg g^{-1}); q_m (mg g^{-1}); k_1 (min^{-1}); k_2 (g mg^{-1} min^{-1}); K_L (L mg^{-1}); K_F (mg$^{1-1/n}$ L$^{1/n}$ g^{-1}); K_S (L g^{-1}); K_{RP} (L g^{-1}); α_{RP}(L mg^{-1})									

The FTIR-ATR results for PS800-10NaOH-HCl show that the carbonate ions present in PS800-10NaOH vanished after washing with HCl (Figure 23a). Also, the adsorption results for PS800-10NaOH-HCl shown that the second “plateau” present in the PS800-10NaOH isotherm disappeared and the first “plateau” lightly increased the adsorption capacity (around 27 mg g^{-1}). Hence, for lower residual concentration of fluoxetine-HCl, the adsorption capacity has slightly increased. Moreover, it can be seen that the kinetic of the process has improved significantly, namely, the rate constant, k_2, of the pseudo-second order model, for PS800-10NaOH-HCl is 20.8 times higher than the k_2 of PS800-10NaOH. These results mean that, in this this case, the carbonates were not favorable to a quick adsorption.

Is interesting to notice that the adsorption capacity of PS800-10NaOH-HCl is similar to the adsorption capacity of PS800-10$ZnCl_2$. The surface area of PS800-10NaOH-HCl is not known but is probably higher than the one of PS800-10NaOH. Also, the presence of mesopores, or even maybe of macropores, can influence the adsorption of fluoxetine on the produced carbons (Al-Degs et al., 2005; Hartmann, 2005), namely in PS800-10, PS800-10KOH and PS800-10NaOH that have about 50% (the two former) and 75% (the latter) of other porosity than micropores.

The main mechanisms proposed in the literature for adsorption of organic molecules involve electrostatic interactions (when the adsorbate is an electrolyte), chemical interaction between the adsorbate molecule and functional groups of the carbons, dispersive interactions between the π delocalized electrons at the carbon basal sites and the π electrons of aromatic structure of the adsorbate, hydrophobic interactions, and molecular sieving (Girods et al., 2009; Kushwaha et al., 2013; Moreno-Castilla, 2004; Nabais et al., 2008). One more time, Al-Degs et al. (2005) suggest that the magnitude of surface area does not reflect the chemical strength of the carbon.

With the data present in this study is not possibly to propose a mechanism of adsorption, however, some analysis can be made. For instance, since the kinetic data better fit to a PSO model, related to chemisorption, is not probable that the adsorption mechanism involved could be electrostatic interactions. However, some authors consider that the adsorption process is partially physical and partially chemical and that the π-π interactions seem to be dominant in the adsorption of aromatic compounds (Radovic, 1997). In the case of PS800-10, PS800-10KOH and PS800-10NaOH, as fluoxetine is not essentially in the protonated form, here dispersive interactions can take place, such as, interactions between the π electrons of the phenyl ring of fluoxetine and the π electrons of the graphitic structure of the carbon material. Also, it has been seen that mesoporosity and pore size distribution can have an important role in the adsorption mechanism (Al-Degs et al., 2004; Kushwaha et al., 2013; Nabais et al., 2008). Yet, to propose a mechanism of adsorption is necessary to know more specific characteristics of the carbon materials, namely the type of carbonates present, and of fluoxetine-HCl and the possible interactions between these molecules.

From the practical point of view, another interesting fact is the concentration of carbon needed to complete removal of the solute from solution. It is observed that the concentration of adsorbent needed to achieve a complete removal is higher for PS800-10, PS800-10KOH and PS800-10NaOH (Figure 25 b, c and d). Although PS800-10ZnCl$_2$ (Figure 25 e) reach the complete removal at a higher concentration than the reference carbon, PBFG4 (Figure 25 a), require a lower concentration than the former three carbons. The same happens for PS800-10NaOH-HCl (Figure 25 f).

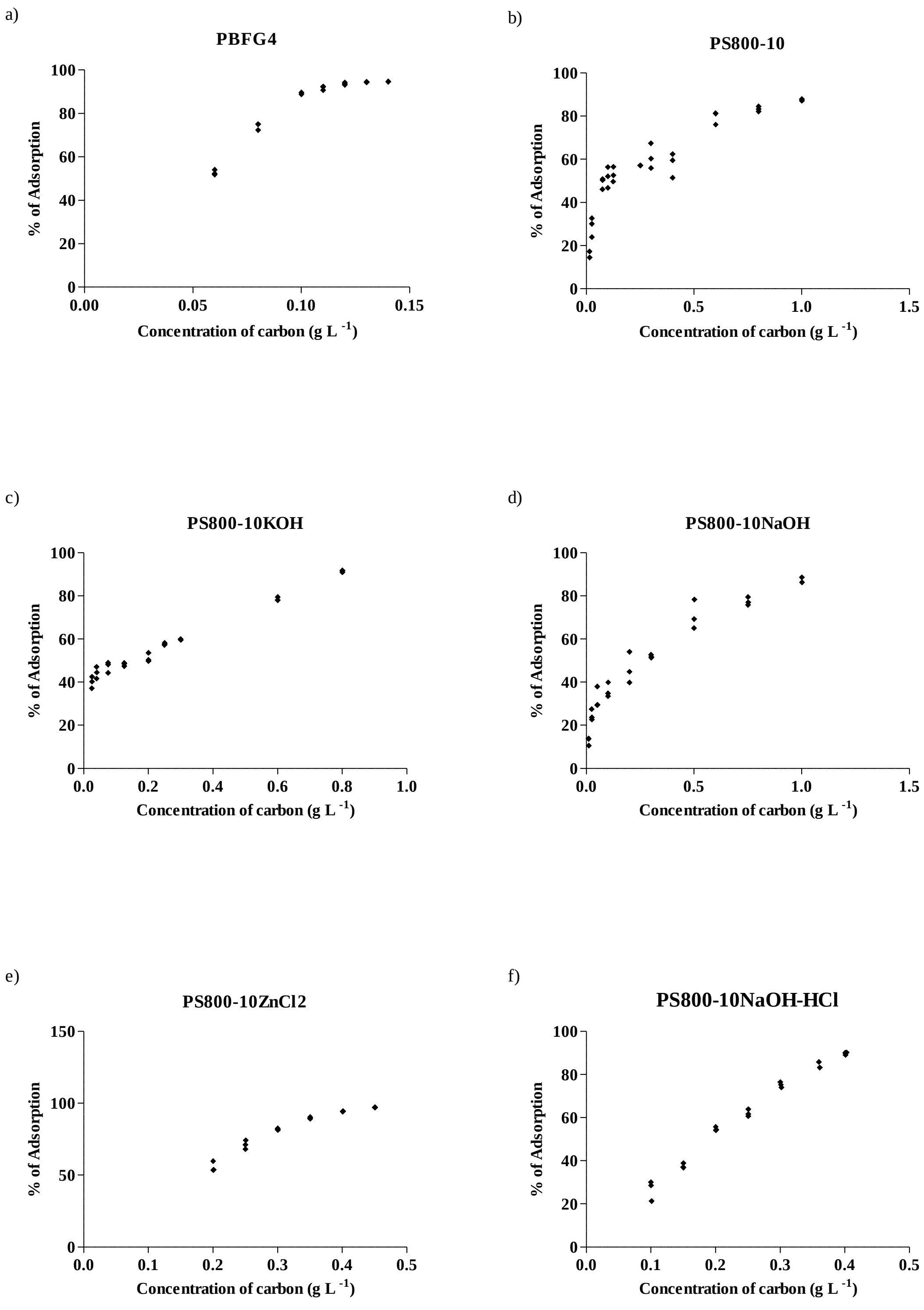

Figure 25 – Percentage of adsorption as a function of the concentration of adsorbent for: a) PBFG4; b) PS800-10; c) PS800-10KOH; d) PS800-10NaOH; e) PS800-10ZnCl$_2$ and f) PS800-10NaOH-HCl.

4. CONCLUSIONS AND FUTURE TRENDS

Different carbons were produced using primary sludge from a paper mill industry as starting material. These carbons were produced by pyrolysis (PS800-10) and by chemical activation prior to pyrolysis using $ZnCl_2$, KOH and NaOH as chemical agents (PS800-10$ZnCl_2$, PS800-10KOH and PS800-10NaOH, respectively). From this work we can conclude that the produced carbons with the chosen experimental conditions, although do not give rise to typical activated carbons, that is, carbons with the distinctive characteristics of the activated carbons, with the exception of PS800-10$ZnCl_2$ which shows an enhancement in surface area and a good microporosity, they were able to remove fluoxetine-HCl from aqueous solution to different extents. The adsorption capacities obtained for the carbons PBFG4, PS800-10, PS800-10KOH, PS800-10NaOH and PS800-10$ZnCl_2$ were 96.2 mg g^{-1}, 120.4 mg g^{-1}, 191.6 mg g^{-1}, 136.6 mg g^{-1}, and 28.4 mg g^{-1}, respectively. Among these carbons, PS800-10$ZnCl_2$, which showed an enhanced surface area and a developed microporosity, displayed comparable physical properties to those of commercial activated carbons.

Different types of isotherms, L and S types, were obtained for the adsorption of fluoxetine-HCl in the different carbon materials, which indicates different adsorption mechanisms. The presence of carbonates in the carbons has influence in the PZC values of the carbons and in the pH of the solution affecting the ionized form of fluoxetine-HCl and then the adsorption mechanism. The carbons that present carbonates (PS800-10, PS800-10KOH and PS800-10NaOH) present an S or H type isotherm and a high adsorption capacity for high concentration with the appearance of a second plateau in the isotherms, corresponding to lateral interactions between adsorbate molecules. However, at low concentration of fluoxetine-HCl, the adsorption capacity that is related with the interaction of these molecules with the carbon surface is low. On the other hand, PS800-10$ZnCl_2$ present a specific surface area in the same order of magnitude of the reference carbon (PBFG4), being about only 30% lower. However, although his adsorption capacity is higher than PS800-10, PS800-10KOH and PS800-10NaOH at the first plateau, is not as good as the reference carbon, being around 70% lower than the latter. Moreover, using HCl in the washing step removes the carbonates, as shown in PS800-10NaOH-HCl and the second plateau of the isotherm disappears. In addition the adsorption capacity of the first plateau increases just a little, approaching the adsorption capacity of PS800-10$ZnCl_2$. More important is the kinetics that is much quicker in PS800-10NaOH-HCl than in all the other carbons.

This study shows the importance of the effect of pH in adsorption mechanism. For fluoxetine-HCl, a solution with a pH close to the pK_a value of this compound seems to benefit the adsorption at high concentration.

In conclusion, although PS800-10, PS800-10KOH and PS800-NaOH did not show a high adsorption capacity at low equilibrium concentrations of fluoxetine-HCl, their relative large “adsorption capacity” at higher equilibrium concentrations may make these materials appropriate for the treatment of concentrated waters, such as effluents from the pharmaceutical industry.

On the whole, it has been shown that the production of activated carbons from primary sludge from the paper pulp industry may be a possible way for the management and valorisation of such wastes. In any case, further studies should be done trying to improve the characteristics of the final carbons, for instance: testing others ratios (w/w) of precursor/activating agent; changing the mixing procedure; varying the conditions of pyrolysis (such as the residence time); and functionalization of the surface.

5. REFERENCES

Ahmad, A., Loh, M., Aziz, J., 2007. Preparation and characterization of activated carbon from oil palm wood and its evaluation on Methylene blue adsorption. Dyes and Pigments 75, 263-272.

Ahmed, M.J., Dhedan, S.K., 2012. Equilibrium isotherms and kinetics modeling of methylene blue adsorption on agricultural wastes-based activated carbons. Fluid Phase Equilibria 317, 9-14.

Al-Degs, Y.S., El-Barghouthi, M.I., Khraisheh, M.A., Ahmad, M.N., Allen, S.J., 2004. Effect of Surface Area, Micropores, Secondary Micropores, and Mesopores Volumes of Activated Carbons on Reactive Dyes Adsorption from Solution. Separation Science and Technology 39, 97-111.

Al-Degs, Y.S., El-Barghouthi, M.I., Khraisheh, M.A., Ahmad, M.N., Allen, S.J., 2005. Effect of Surface Area, Micropores, Secondary Micropores, and Mesopores Volumes of Activated Carbons on Reactive Dyes Adsorption from Solution. Separation Science and Technology 39, 97-111.

Alcañiz-Monge, J., Illan-Gomez, M.J., 2008. Insight into hydroxides-activated coals: chemical or physical activation? J Colloid Interface Sci 318, 35-41.

Atta-Politou, J., Skopelitis, I., Apatsidis, I., Koupparis, M., 2001. In vitro study on fluoxetine adsorption onto charcoal using potentiometry. European Journal of Pharmaceutical Sciences 12, 311–319.

Azargohar, R., Dalai, A.K., 2006. Biochar As a Precursor of Activated Carbon. Applied Biochemistry and Biotechnology 129-132, 762-773.

Azargohar, R., Dalai, A.K., 2008. Steam and KOH activation of biochar: Experimental and modeling studies. Microporous and Mesoporous Materials 110, 413-421.

Azizian, S., 2004. Kinetic models of sorption: a theoretical analysis. J Colloid Interface Sci 276, 47-52.

Bagheri, H., Zandi, O., Aghakhani, A., 2011. Extraction of fluoxetine from aquatic and urine samples using sodium dodecyl sulfate-coated iron oxide magnetic nanoparticles followed by spectrofluorimetric determination. Analytica Chimica Acta 692, 80-84.

Bandosz, T.J., 2006. Activated Carbon Surfaces in Environmental Remediation, first ed. Elsevier, New York.

Bansal, R.C., Goyal, M., 2005. Activated Carbon Adsorption. Taylor & Francis, U.S.A.

Bell, K.Y., Wells, M.J.M., Traexler, K.A., Pellegrin, M.-L., Morse, A., Bandy, J., 2011. Emerging Pollutants. Water Environment Research 83, 1906-1984.

Bond, R.L., 1967. Porous Carbon Solids. Academic Press, London.

Bonenfant, D., Mimeault, M., Niquette, P., Hausler, R., 2012. Adsorption study of a commonly used antidepressant drug, fluoxetine hydrochloride, onto a crosslinked beta-cyclodextrin-carboxymethylcellulose polymer. Water Sci Technol 66, 224-230.

Brooks, B.W., Foran, C.M., Richards, S.M., Weston, J., Turner, P.K., Stanley, J.K., Solomon, K.R., Slattery, M., La Point, T.W., 2003. Aquatic ecotoxicology of fluoxetine. Toxicology Letters 142, 169-183.

Brunauer, S., Emmett, P.H., Teller, E., 1938. Adsorption of Gases in Multimolecular Layers. Journal of the American Chemical Society 60, 309-319.

Burrows, H.D., Pereira, M.M., 2006. Química Síntese e Estrutura- uma aborgadem prática. Escolar Editora, Portugal.

Butt, H.J., Graf, K., Kappl, M., 2003. Physics and Chemistry of Interfaces. WILEY-VCH GmbH & Co. KGaA, Weinheim.

Calisto, V., 2011. Environmental occurrence and fate of psychiatric pharmaceuticals, Departamento de Química. Universidade de Aveiro.

Calisto, V., Ferreira, C.I.A., Santos, S.M., Gil, M.V., Otero, M., Esteves, V.I., 2014. Production of adsorbents by pyrolysis of paper mill sludge and application on the removal of citalopram from water. Bioresour Technol 166, 335–344.

Cao, Q., Xie, K.C., Lv, Y.K., Bao, W.R., 2006. Process effects on activated carbon with large specific surface area from corn cob. Bioresour Technol 97, 110-115.

Chingombe, P., Saha, B., Wakeman, R.J., 2006. Effect of surface modification of an engineered activated carbon on the sorption of 2,4-dichlorophenoxy acetic acid and benazolin from water. J Colloid Interface Sci 297, 434-442.

Coates, J., 2000. Interpretation of Infrared Spectra, A Practical Approach. John Wiley & Sons Ltd, Chichester.

Cooney, D.O., Thomason, R., 1997. Adsorption of Fluoxetine HCl by Activated Charcoal. Journal of Pharmaceutical Sciences 85, 642-644.

Dabrowski, A., 2001. Adsorption - from theory to practice. Advances in Colloid and Interface Science 93, 135-224.

Dabrowski, A., Podkoscielny, P., Hubicki, Z., Barczak, M., 2005. Adsorption of phenolic compounds by activated carbon--a critical review. Chemosphere 58, 1049-1070.

Debrassi, A.L., M. C. T.; Rodrigues, C. A., 2011. Adsorção do Corante Vermelho Congo por Derivados da O-Carboximetilquitosana Hidrofobicamente Modificados. Quim. Nova 34, 764-770.

Desta, M.B., 2013. Batch Sorption Experiments: Langmuir and Freundlich Isotherm Studies for the Adsorption of Textile Metal Ions onto Teff Straw (Eragrostis tef) Agricultural Waste. Journal of Thermodynamics 2013, 1-6.

Devi, P., Saroha, A.K., 2013. Effect Of Temperature On Biochar Properties During Paper Mill Sludge Pyrolysis. International Journal of ChemTech Research 5 682-687.

Flores, J.R., Nevado, J.J., Penalvo, G.C., Diez, N.M., 2005. Development and validation method for determination of fluoxetine and its main metabolite norfluoxetine by nonaqueous capillary electrophoresis in human urine. Talanta 65, 163-171.

Foo, K.Y., Hameed, B.H., 2010. Insights into the modeling of adsorption isotherm systems. Chemical Engineering Journal 156, 2-10.

Franz, M., Arafat, H.A., Pinto, N.G., 2000. Effect of chemical surface heterogeneity on the adsorption mechanism of dissolved aromatics on activated carbon. Carbon 38, 1807–1819.

Fuqiang, L., Mingfang, X., Zhenghao, F., Jinlong, C., Aimin, L., 2007. Adsorption selectivity of salicylic acid and 5-sulfosalicylic acid onto hypercrosslinked polymeric adsorbents. Front. Environ. Sci. Engin. 1, 73-78.

Giles, C.H., Macewan, T.H., Nakhwa, S.N., Smith, D., 1960. Studies in Adsorption. Part XI. A System of Classification of Solution Adsorption Isotherms, and its Use in Diagnosis of Adsorption Mechanisms and in Measurement of Specific Surface Areas of Solids. Journal of the Chemical Society 01.

Girods, P., Dufour, A., Fierro, V., Rogaume, Y., Rogaume, C., Zoulalian, A., Celzard, A., 2009. Activated carbons prepared from wood particleboard wastes: characterisation and phenol adsorption capacities. J Hazard Mater 166, 491-501.

Granström, M., 2009. Cellulose Derivatives: Synthesis, Properties and Applications, Department of Chemistry. University of Helsinki, Helsinki.

Gregg, S.J., Sing, K.S., 1991. Adsorption, Surface Area and Porosity, 2nd ed. Academic Press, London.

Guilarduci, V.V.S., Mesquita, J.P., Martelli, P.B., Gorgulho, H.F., 2006. Adsorção de fenol sobre carvão ativado em meio alcalino. Quim. Nova 29, 1226-1232.

Guo, Y., Rockstraw, D.A., 2006. Physical and chemical properties of carbons synthesized from xylan, cellulose, and Kraft lignin by H3PO4 activation. Carbon 44, 1464-1475.

Hadi, M., Samarghandi, M.R., McKay, G., 2010. Equilibrium two-parameter isotherms of acid dyes sorption by activated carbons: Study of residual errors. Chemical Engineering Journal 160, 408-416.

Hamdaoui, O., Naffrechoux, E., 2007a. Modeling of adsorption isotherms of phenol and chlorophenols onto granular activated carbon. Part I. Two-parameter models and equations allowing determination of thermodynamic parameters. J Hazard Mater 147, 381-394.

Hamdaoui, O., Naffrechoux, E., 2007b. Modeling of adsorption isotherms of phenol and chlorophenols onto granular activated carbon. Part II. Models with more than two parameters. J Hazard Mater 147, 401-411.

Hameed, B.H., Mahmoud, D.K., Ahmad, A.L., 2008. Equilibrium modeling and kinetic studies on the adsorption of basic dye by a low-cost adsorbent: coconut (Cocos nucifera) bunch waste. J Hazard Mater 158, 65-72.

Hartmann, M., 2005. Ordered Mesoporous Materials for Bioadsorption and Biocatalysis. Chem. Mater 17, 4577-4593.

Hassan, A.F., Abdel-Mohsen, A.M., Fouda, M.M., 2014. Comparative study of calcium alginate, activated carbon, and their composite beads on methylene blue adsorption. Carbohydr Polym 102, 192-198.

Hayashi, J., Kazehaya, A., Muroyama, K., Watkinson, A.P., 2000. Preparation of activated carbon from lignin by chemical activation. Carbon 38, 1873-1878.

Ho, Y.S., 2006. Review of second-order models for adsorption systems. J Hazard Mater 136, 681-689.

Ho, Y.S., McKay, G., 1999. Pseudo-second order model for sorption processes. Process Biochemistry 34 451–465.

Infarmed, Estatística do Medicamento. Ministério da Saúde, http://labvirtual.eq.uc.pt/siteJoomla/index.php?Itemid=450&id=188&option=com_content &task=view.

IUPAC, 2012. Compendium of Chemical Terminology. Gold Book. Version 2.3.2.

Junior, M.Â.S., 2004. Ativação Química do Carvão de Casca de Arroz Utilizando NaOH, Centro de Ciências Exatas. Universidade Federal do Espírito Santo.

Karakoyun, N., Kubilay, S., Aktas, N., Turhan, O., Kasimoglu, M., Yilmaz, S., Sahiner, N., 2011. Hydrogel–Biochar composites for effective organic contaminant removal from aqueous media. Desalination 280, 319-325.

Khalil, H.P.S.A., Jawaid, M., Firoozian, P., Rashid, U., Islam, A., Akil, H.M., 2013. Activated Carbon from Various Agricultural Wastes by Chemical Activation with KOH: Preparation and Characterization. Journal of Biobased Materials and Bioenergy 7, 708-714.

Khalili, N.R., Campbell, M., Sandi, G., Golas, J., 2000. Production of micro- and mesoporous activated carbon from paper mill sludge - I. Effect of zinc chloride activation. Carbon 38.

Kim, K.H., Kim, J.Y., Cho, T.S., Choi, J.W., 2012. Influence of pyrolysis temperature on physicochemical properties of biochar obtained from the fast pyrolysis of pitch pine (Pinus rigida). Bioresour Technol 118, 158-162.

Kobayashi, H., Ito, Y., Komanoya, T., Hosaka, Y., Dhepe, P.L., Kasai, K., Hara, K., Fukuoka, A., 2011. Synthesis of sugar alcohols by hydrolytic hydrogenation of cellulose over supported metal catalysts. Green Chemistry 13, 326.

Kumar, K.V., Porkodi, K., Rocha, F., 2008. Comparison of various error functions in predicting the optimum isotherm by linear and non-linear regression analysis for the sorption of basic red 9 by activated carbon. J Hazard Mater 150, 158-165.

Kushwaha, S., Soni, H., Ageetha, V., Padmaja, P., 2013. An Insight Into the Production, Characterization, and Mechanisms of Action of Low-Cost Adsorbents for Removal of Organics From Aqueous Solution. Critical Reviews in Environmental Science and Technology 43, 443-549.

Larsson, P.T., Hult, E., Wickholm, K., Pettersson, E., Iversen, T., 1999. CP/MAS ^{13}C-NMR spectroscopy applied to structure and interaction studies on cellulose I. Solid State Nuclear Magnetic Resonance 15, 31–40

Lichtfouse, E., Schwarzbauer, J., Robert, D., 2012. Environmental Chemistry for a Sustainable World. Springer, New York.

Lillo-Rodenas, M.A., Cazorla-Amoros, D., Linares-Solano, A., 2003. Understanding chemical reactions between carbons and NaOH and KOH. An insight into the chemical activation mechanism. Carbon 41, 267–275.

Lillo-Ródenas, M.A., Marco-Lozar, J.P., Cazorla-Amorós, D., Linares-Solano, A., 2007. Activated carbons prepared by pyrolysis of mixtures of carbon precursor/alkaline hydroxide. Journal of Analytical and Applied Pyrolysis 80, 166-174.

Lima, D.L., Calisto, V., Esteves, V.I., 2011. Adsorption behavior of 17alpha-ethynylestradiol onto soils followed by fluorescence spectral deconvolution. Chemosphere 84, 1072-1078.

Limousin, G., Gaudet, J.P., Charlet, L., Szenknect, S., Barthès, V., Krimissa, M., 2007. Sorption isotherms: A review on physical bases, modeling and measurement. Applied Geochemistry 22, 249-275.

Liu, Y.a.S.L., 2008. From Langmuir Kinetics to First- and Second-Order Rate Equations for Adsorption. Langmuir 24, 11625-11630.

Maas, J.H.v.d., 1972. Basic Infrared Spectroscopy, second ed. Heyden & Son Ltd, Great Britain.

Machado, F.M., 2011. Adsorção do corante sintético vermelho reativo 194 de efluente aquoso por nanotubos de carbono de paredes múltiplas e por carvão ativo, Escola de engenharia. Universidade Federal do Rio Grande do Sul, Rio Grande do Sul.

Marczewski, A.W., 2007. Kinetics and equilibrium of adsorption of organic solutes on mesoporous carbons. Applied Surface Science 253, 5818-5826.

Marsh, H., Rodríguez-Reinoso, F., 2006. Activated Carbon, First ed. Elsevier, England.

McElroy, J.A., 2005. Adsorption of substituted aromatic compounds by activated carbon: a mechanistic approach to quantitative structure activity relationships. University of Florida.

Miller, J.N., Miller, J.C., 2010. Statistics and Chemometrics for Analytical Chemistry, Sixth ed. Prentice Hall, England.

Moreno-Castilla, C., 2004. Adsorption of organic molecules from aqueous solutions on carbon materials. Carbon 42, 83-94.

Nabais, J.M.V., Mouquinho, A., Galacho, C., Carrott, P.J.M., Ribeiro Carrott, M.M.L., 2008. In vitro adsorption study of fluoxetine in activated carbons and activated carbon fibres. Fuel Processing Technology 89, 549-555.

Nevskaia, D.M., Sepulveda-Escribano, A., Guerrero-Ruiz, A., 2001. Surface properties of activated carbons in relation to their ability to adsorb nonylphenol aqueous contaminant. Physical Chemistry Chemical Physics 3, 463-468.

Patricia, L.L., Quinlivan, A., Knappe, D.R.U., 2002. Effects of activated carbon surface chemistry and pore structure on the adsorption of organic contaminants from aqueous solution. Carbon 40, 2085–2100.

Pereira, R.G., 2012. Síntese de carvões ativados a partir de resíduos agroindustriais e sua aplicação na adsorção de proteínas do soro do leite. Universidade Estadual do Sudoeste da Bahia, Brasil.

Petrova, B., Budinova, T., Tsyntsarski, B., Kochkodan, V., Shkavro, Z., Petrov, N., 2010. Removal of aromatic hydrocarbons from water by activated carbon from apricot stones. Chemical Engineering Journal 165, 258-264.

Pietrzak, R., Nowicki, P., Kazmierczak, J., Kuszynska, I., Goscianska, J., Przepiórski, J., 2013. Comparison of the effects of different chemical activation methods on properties of carbonaceous adsorbents obtained from cherry stones Chemical Engineering Research and Design.

Prola, L.D.T., Acayanka, E., Lima, E.C., Umpierres, C.S., Vaghetti, J.C.P., Santos, W.O., Laminsi, S., Djifon, P.T., 2013. Comparison of Jatropha curcas shells in natural form and treated by non-thermal plasma as biosorbents for removal of Reactive Red 120 textile dye from aqueous solution. Industrial Crops and Products 46, 328-340.

Qi, S., Schideman, L.C., 2008. An overall isotherm for activated carbon adsorption of dissolved natural organic matter in water. Water Res 42, 3353-3360.

Qiu, H., Lv, L., Pan, B.-c., Zhang, Q.-j., Zhang, W.-m., Zhang, Q.-x., 2009. Critical review in adsorption kinetic models. Journal of Zhejiang University SCIENCE A 10, 716-724.

Radjenovic, J., Petrovic, M., Barceló, D., 2009. Fate and distribution of pharmaceuticals in wastewater and sewage sludge of the conventional activated sludge (CAS) and advanced membrane bioreactor (MBR) treatment. Water Res 43, 831-841.

Radovic, L.R., 2008. Chemistry and Physics of Carbon. CRC Press, U.S.A.

Radovic, R.L.S., I. F.; Ume, J. I.; Menéndez, J. A.; Leon & Leon, C. A.; Scaroni, A. W., 1997. An Experimental and Theoretical Study of the Adsorption of Aromatics Possessing Electron-withdrawing and Electron-donating Functional Groups by Chemical Modified Activated Carbons. Carbon 35, 1339-1348.

Rossner, A., Snyder, S.A., Knappe, D.R., 2009. Removal of emerging contaminants of concern by alternative adsorbents. Water Res 43, 3787-3796.

Rouquerol, F., Rouquerol, J., Sing, K.S.W., Llewellyn, P., Maurin, G., 2014. Adsorption by Powders and Porous Solids - Principles, Methodology and Applications, Second ed. Academic Press, Poland.

Sekar, M., Sakthi, V., Rengaraj, S., 2004. Kinetics and equilibrium adsorption study of lead(II) onto activated carbon prepared from coconut shell. J Colloid Interface Sci 279, 307-313.

Sevilla, M., Fuertes, A.B., 2009. The production of carbon materials by hydrothermal carbonization of cellulose. Carbon 47, 2281-2289.

Sirimuangjinda, A., Hemra, K., Atong, D., Pechyen, C., 2013. Comparison on Pore Development of Activated Carbon Produced from Scrap Tire by Potassium Hydroxide and Sodium Hydroxide for Active Packaging Materials. Key Engineering Materials 545, 129-133.

Srinivasakannan, C., Bakar, M.Z.A., 2004. Production of activated carbon from rubber wood sawdust. Biomass and Bioenergy 27, 89-96.

Tang, M.M., Bacon, R., 1964. Carbonbization of Cellulose Fbers - I. Low Temperature Pyrolysis. Carbon 2, 211-220.

Tay, T., Ucar, S., Karagoz, S., 2009. Preparation and characterization of activated carbon from waste biomass. J Hazard Mater 165, 481-485.

Yang, H., Yan, R., Chen, H., Lee, D.H., Zheng, C., 2007. Characteristics of hemicellulose, cellulose and lignin pyrolysis. Fuel 86, 1781-1788.

Yang, R.T., 2003. Adsorbents: Fundamentals and Applications. John Wiley & Sons, Inc., New Jersey.

Yu, M., Gong, H., Chen, Z., Zhang, M., 2013. Adsorption characteristics of activated carbon for siloxanes. Journal of Environmental Chemical Engineering 1, 1182-1187.

Zhu, B.Y., Gu, T., 1989. General Isotherm Equation for Adsorption of Surfactants at Solid/Liquid Interfaces. J. Chem. Soc. 85, 3813-3817.